Covariant and self-consistent vertex corrections for pions and isobars in nuclear matter

C. L. Korpa
Department of Theoretical Physics, University of Pecs, Ifjusag u. 6, H-7624 Pecs, Hungary

M. F. M. Lutz and F. Riek*
Gesellschaft für Schwerionenforschung (GSI), Planck Str. 1, D-64291 Darmstadt, Germany
(Received 26 September 2008; published 7 August 2009)

We evaluate the pion and isobar propagators in cold nuclear matter self-consistently applying a covariant form of the isobar-hole model. Migdal's vertex correction effects are considered systematically in the absence of phenomenological soft form factors. Saturated nuclear matter is modeled by scalar and vector mean fields for the nucleon. It is shown that the short-range dressing of the $\pi N\Delta$ vertex has a significant effect on the pion and isobar properties. Using realistic parameters sets we predict a downward shift of about 50 MeV for the Δ resonance at nuclear saturation density. The pionic soft modes are much less pronounced than in previous studies.

DOI: 10.1103/PhysRevC.80.024901 PACS number(s): 25.20.Dc, 24.10.Jv, 21.65.−f, 13.75.Gx

I. INTRODUCTION

The theoretical approaches for the nuclear pion dynamics [1–25] followed so far can be put into different categories. All works acknowledge and consider the important role of short-range correlation effects. However, there is no common consensus about their absolute strength. The latter depends decisively on the subtle details of the considered approach. For instance the nonrelativistic computations [13,15,18] obtain contrasted results for the pion properties in cold nuclear matter. With few exceptions [6,11,17,20,21] nonrelativistic many-body techniques are applied. Also works that incorporate the feedback effect of a dressed pion propagator, that depends sensitively on the isobar propagator itself, on the isobar self-energy are in the minority [5,14,16,21–23,25]. It has been found that self-consistency is a crucial effect for the nuclear $\pi N\Delta$ dynamics. Moreover, the in-medium isobar propagator should be used in the computation of the isobar-hole contribution building up the short-ange correlation effects [15,21,22]. In the early works that addressed self-consistency issues [14,16] a quite soft phenomenological form factor was used. This implies a strong and artificial suppression of pionic soft modes with large momentum that dominate the isobar width [21]. The use of such soft form factors explains why in [14,16] quite conventional isobar properties [30] were obtained without the inclusion of vertex correction effects in the isobar self-energy. The use of soft form factors suppresses the in-medium mass and width shifts of the isobar significantly. Noteworthy is the work of Ref. [15], in which isobar properties were computed without relying on soft form factors. The important role of a hard factors in the nuclear $\pi N\Delta$ dynamics was pointed out in [5]. One may conclude that a description of isobar properties [14,16,21–23,25] that relies on soft form factors should not be considered microscopic unless one includes a strong density, energy, and momentum dependence in the form factor.

A further possibly important aspect is the splitting of the isobar modes in nuclear matter [7,15,21]. An isobar moving through nuclear matter manifests itself in terms of longitudinal and transverse modes described by distinct spectral functions. The splitting of the two modes was found to be small in [7,21]. In contrast, in [15] sizable effects were found depending, however, on the precise structure of the form factors used. Notwithstanding, further clarification on the form of the isobar self-energy in nuclear matter is needed. This is of particular relevance for instance in applications to heavy-ion reactions [25].

Recently it was demonstrated [20] that a covariant form of the isobar-hole model differs significantly from nonrelativistic versions thereof [4,6,8]. Relativistic corrections are not important everywhere in phase space. As a striking example recall the behavior of the nucleon-hole contribution to the pion self-energy. A proper relativistic treatment leads to a result proportional to $\omega^2 - \vec{q}^{\,2}$, with the pion energy and momentum ω and $\vec{q}$, respectively [6,8,20]. In contrast, a nonrelativistic evaluation provides a factor $\vec{q}^{\,2}$ only [4]. Obviously, the nonrelativistic expression is justified only in a small subspace of phase space. Paying contribute to this observation various prescriptions (see, e.g., [15]) were suggested in the literature. One may speculate that the incompatible treatment of such effects is an important source for conflicting sets of Migdal parameters used in the literature [6,15,19,22].

Though it should be possible to incorporate relativistic effects in a perturbative manner with possible partial summations required, we argue that it is more economical to perform computations that are strictly covariant. Applying the projector techniques developed recently [20,26–28] it is straightforward to perform such calculations. In [21] a first manifest covariant and self-consistent computation of the pion self-energy was presented. The incorporation of scalar and vector mean fields for the nucleon was worked out recently in [28] at hand of the nuclear antikaon dynamics.

The purpose of this work is to extend the previous studies of two of us [20,21]. We compute the isobar self-energy in a covariant and self consistent manner generalizing the covariant isobar-hole model of [20]. Vertex correction effects

*Current affiliation: Cyclotron Institute and Physics Department, Texas A&M University, College Station, Texas H-77843-3366, USA.

as well as the longitudinal and transverse isobar modes are treated consistently. Results will be presented for a range of parameters centered around a parameter set that was found to be compatible in [29] with the nuclear photo-absorption data [31]. The effect of various approximations is discussed and illustrated comprehensively.

II. COVARIANT ISOBAR-HOLE MODEL

We specify the isobar-hole model in its covariant form [19,20]. The interaction of pions with nucleons and isobars is modelled by the leading order vertices

$$\mathcal{L} = \frac{f_N}{m_\pi}\,\bar\psi\,\gamma_5\,\gamma^\mu\,(\partial_\mu\vec\pi\,)\,\vec\tau\,\psi + \frac{f_\Delta}{m_\pi}\,(\bar\psi^\mu(\partial_\mu\vec\pi\,)\,\vec T\,\psi + \text{h.c.}), \tag{1}$$

where we use $T_i^\dagger\,T_j = \delta_{ij} - \tau_i\,\tau_j/3$ and $f_N = 0.988$ and $f_\Delta = 1.85$ in this work. Short-range correlation effects are modelled using the covariant form of the Migdal interaction vertices as introduced in [19,20]:

$$\begin{aligned}\mathcal{L}_{\text{Migdal}} &= g'_{11}\frac{f_N^2}{m_\pi^2}\,(\bar\psi\,\gamma_5\,\gamma_\mu\,\vec\tau\,\psi)\,(\bar\psi\,\gamma_5\,\gamma^\mu\,\vec\tau\,\psi)\\ &\quad + g'_{22}\frac{f_\Delta^2}{m_\pi^2}((\bar\psi_\mu\,\vec T\,\psi)\,(\bar\psi\,\vec T^\dagger\psi^\mu)\\ &\quad + ((\bar\psi_\mu\,\vec T\,\psi)\,(\bar\psi^\mu\,\vec T\,\psi) + \text{h.c.}))\\ &\quad + g'_{12}\frac{f_N\,f_\Delta}{m_\pi^2}\,(\bar\psi\,\gamma_5\,\gamma_\mu\,\vec\tau\,\psi)((\bar\psi^\mu\vec T\,\psi) + \text{h.c.}),\end{aligned} \tag{2}$$

where it is understood that the local vertices are to be used at the Hartree level. The Fock contribution can be cast into the form of a Hartree contribution by a simple Fierz transformation. Therefore it only renormalizes the coupling strength in Eq. (2) and can be omitted here. The Lagrangian densities (1), (2) are effective in the sense that we consider their coupling constants as functions of the nuclear density. This is justified since we do not incorporate the physics of higher lying baryon resonances nor further mesonic degrees of freedom such as the vector mesons explicitly. Integrating out more massive degrees freedom leads to a density dependence of the coupling constants necessarily, which however, is expected to be quite smooth due to high-mass nature of the modes treated implicitly.

Unfortunately, there is yet no set of Migdal parameters universally accepted. For instance, the computation [15] used the universal values $g'_{11} = g'_{12} = g'_{22} = 0.60$, based on a study of isobar properties. Universal values for the Migdal parameters were suggested first in [1]. Nakano *et al.* [19] deduce the constraint $g'_{11} = 0.585$ together with $g'_{12} = 0.191 + 0.051\,g'_{22}$ insisting on the empirical quenching factor $Q = 0.9$ of the Gamow-Teller resonance [32]. Their consideration assumes that the quenching results exclusively from a mixing of the nucleon-hole and the isobar-hole state. In our work the parameters g'_{ij} are varied around the values $g'_{11} \simeq 1.0$, $g'_{22} = g'_{12} \simeq 0.4$ obtained from a detailed analysis of the nuclear photo-absorption data [29].

Our studies will be based on the in-medium nucleon propagator parameterized in terms of scalar and vector mean fields:

$$\begin{aligned}\mathcal{S}(p,u) &= \frac{1}{\not p - \Sigma_V^N\,\not u - m_N + i\,\epsilon} + \Delta S(p,u),\\ m_N &= m_N^{\text{vac}} - \Sigma_N^S,\\ \Delta S(p,u) &= 2\,\pi\,i\,\Theta\big[p\cdot u - \Sigma_V^N\big]\,\delta\big[\big(p - \Sigma_V^N\,u\big)^2 - m_N^2\big]\\ &\quad\times(\not p - \Sigma_V\,\not u + m_N)\,\Theta\big[k_F^2 + p^2 - (u\cdot p)^2\,\big],\end{aligned} \tag{3}$$

where the Fermi momentum k_F specifies the nucleon density ρ with

$$\rho = -2\,\text{tr}\,\gamma_0\int\frac{d^4p}{(2\pi)^4}\,i\,\Delta S(p,u) = \frac{2\,k_F^3}{3\,\pi^2\,\sqrt{1-\vec u^{\,2}/c^2}}. \tag{4}$$

In the rest frame of the bulk with $u_\mu = (1,\vec 0\,)$ one recovers with Eq. (4) the standard result $\rho = 2\,k_F^3/(3\,\pi^2)$. We assume isospin symmetric nuclear matter.

The focus of our work is the study of the in-medium isobar propagator $S_{\mu\nu}(w,u)$, the solution of Dyson's equation

$$\begin{aligned}S_0^{\mu\nu}(w) &= \frac{-1}{\not w - m_\Delta + i\,\epsilon}\\ &\quad\times\left(g^{\mu\nu} - \frac{\gamma^\mu\,\gamma^\nu}{3} - \frac{2\,w^\mu\,w^\nu}{3\,m_\Delta^2} - \frac{\gamma^\mu\,w^\nu - w^\mu\,\gamma^\nu}{3\,m_\Delta}\right),\\ S_{\mu\nu}(w,u) &= S_{\mu\nu}^{(0)}\big(w - \Sigma_V^\Delta\,u\big)\\ &\quad + S_{\mu\alpha}^{(0)}\big(w - \Sigma_V^\Delta\,u\big)\,\Sigma^{\alpha\beta}(w,u)S_{\beta\nu}(w,u),\end{aligned} \tag{5}$$

where we allow for a vector mean field of the isobar.

In nuclear matter the isobar self-energy tensor, $\Sigma_{\mu\nu}(w,u)$, is a quite complicated object which involves the time-like four-vector u_μ characterizing the nuclear matter frame. In order to arrive at a reproduction of the P33 pion-nucleon partial-wave amplitude we allow for a phenomenological energy dependence in the free-space isobar mass. We write

$$m_\Delta = m_\Delta^{\text{vac}}(\sqrt{w^2}\,) - \Sigma_S^\Delta, \tag{6}$$

where we introduce also a scalar mean field Σ_S^Δ for the isobar. At nuclear saturation density we found the values $\Sigma_V^\Delta \simeq -0.25$ GeV and $\Sigma_S^\Delta \simeq -0.11$ GeV to be consistent with the nuclear photo-absorption data in an application of the present covariant and self-consistent many-body approach [29]. Note that latter values are scheme dependent reflecting the particular in-medium processes taken into account explicitly.

Making the assumption that the P33 amplitude is determined completely by the s-channel exchange of the dressed isobar, for a given isobar self-energy the mass function m_Δ^{vac} can be expressed directly in terms of the empirical P33 phase shift. Based on the self-energy to be specified in Sec. V we arrive at the mass function shown in Fig. 1 with a dashed line. The sizable variation of m_Δ^{vac} on $\sqrt{w^2}$ reflects contributions to the P33 amplitude that are characterized by left-hand branch points. The amplitude receives, besides the s-channel isobar exchange, additional contributions as from the nucleon u-channel process. Since the latter contribution

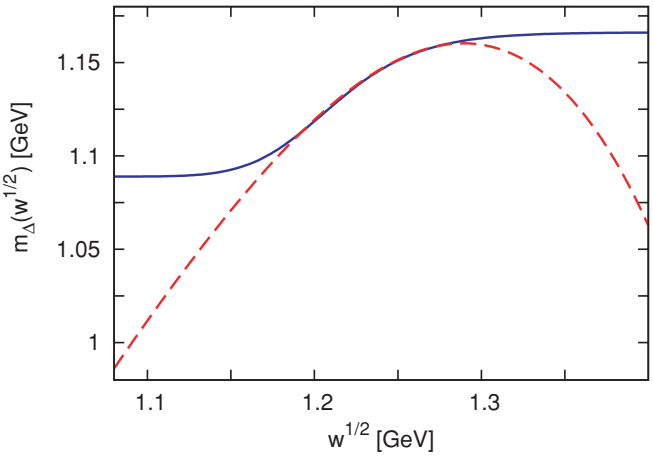

FIG. 1. (Color online) Phenomenological isobar mass functions $m_\Delta^{\rm vac}(\sqrt{w^2})$ that lead to the reproduction of the P33 pion-nucleon scattering amplitude. The dashed (solid) line leads to an exact (approximate) reproduction of the amplitude.

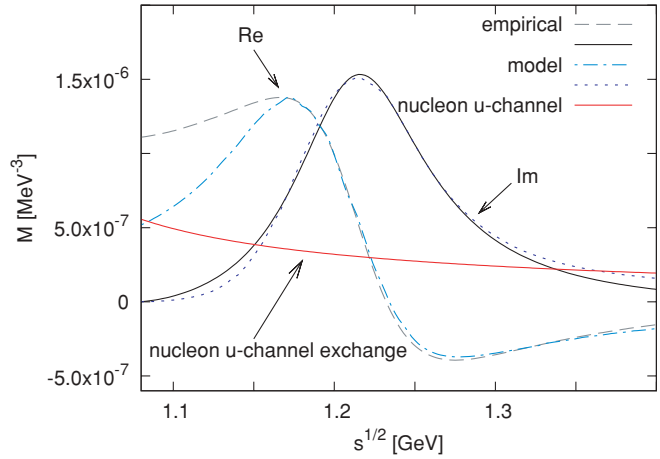

FIG. 2. (Color online) Comparison of the empirical P33 amplitude from [33] with the phenomenological one as implied by Eq. (6) with the solid mass function of Fig. 2. The additional solid line is the contribution of the u-channel nucleon exchange process.

will be considered being implied by Eq. (1), it is not consistent to proceed with the dashed mass function of Fig. 1. A fully consistent approach would require at least the unitarization of the sum of s-channel isobar and u-channel nucleon exchange processes. This is, however, beyond the scope of the present work. In order to correct for the presence of the u-channel nucleon exchange we determine the phenomenological mass function $m_\Delta^{\rm vac}(\sqrt{w^2})$ in the following way: the s-channel isobar contribution is adjusted to reproduce the imaginary part of the P33 partial wave amplitude in the vicinity of the isobar peak. Away from the resonance the mass function is kept constant. The result is shown in Fig. 1 with a solid line. As compared to the dashed line, which reproduces the P33 amplitude exactly, the solid line shows a much reduced variation. This is welcome since the smoother the phenomenological mass function the smaller are the uncertainties implied by the ansatz (6).

The quality of our prescription is illustrated in Fig. 2, where the empirical P33 partial wave amplitude in the convention of [21] is confronted with the phenomenological amplitude. Real and imaginary parts agree well in the resonance region. Significant deviations are noted close to threshold only, where we expect a strong energy dependence from the u-channel contributions. This is confirmed by the additional solid line of Fig. 2 which shows the contribution of the u-channel nucleon exchange process. Close to threshold it is largest almost making up the difference of the empirical and phenomenological amplitude.

III. PION SELF-ENERGY

In this section we evaluate the pion self energy as implied by the interaction (1) for a given isobar propagator $S_{\mu\nu}(w,u)$. The latter will be specified in subsequent sections. The central objects to compute are the nucleon- and isobar-hole loop tensors, $\Pi_{\mu\nu}^{(Nh)}(q,u)$ and $\Pi_{\mu\nu}^{(\Delta h)}(q,u)$, which we define by

$$
\begin{aligned}
\Pi_{\mu\nu}^{(\Delta h)}(q,u) &= \frac{4}{3}\frac{f_\Delta^2}{m_\pi^2}\int\frac{d^4p}{(2\pi)^4}\,i\,\mathrm{tr}\;\Delta S(p,u)S_{\mu\nu}(p+q,u)\\
&\quad+(q_\mu\to-q_\mu),\\
\Pi_{\mu\nu}^{(Nh)}(q,u) &= 2\,\frac{f_N^2}{m_\pi^2}\int\frac{d^4p}{(2\pi)^4}\,i\\
&\quad\times\mathrm{tr}\left(\Delta S(p,u)\,\gamma_5\,\gamma_\mu\,\frac{1}{\not p-\Sigma_V^N\not u+\not q-m_N}\,\gamma_5\,\gamma_\nu\right.\\
&\quad\left.+\frac{1}{2}\Delta S(p,u)\,\gamma_5\,\gamma_\mu\,\Delta S(p+q,u)\,\gamma_5\,\gamma_\nu\right)\\
&\quad+(q_\mu\to-q_\mu),
\end{aligned}
\tag{7}
$$

with the isobar propagator, $S_{\mu\nu}(w,u)$ of Eq. (6), and the in-medium part of the nucleon propagator, $\Delta S(p,u)$ as specified in Eq. (3).

The computation of short-range correlation effects is considerably streamlined upon decomposing the nucleon- and isobar-hole tensors,

$$
\begin{aligned}
\Pi_{\mu\nu}^{(Nh)}(q,u) &= \sum_{i,j=1}^{2}\Pi_{ij}^{(Nh)}(q,u)\,L_{\mu\nu}^{(ij)}(q,u)\\
&\quad+\Pi_T^{(Nh)}(q,u)\,T_{\mu\nu}(q,u),\\
\Pi_{\mu\nu}^{(\Delta h)}(q,u) &= \sum_{i,j=1}^{2}\Pi_{ij}^{(\Delta h)}(q,u)\,L_{\mu\nu}^{(ij)}(q,u)\\
&\quad+\Pi_T^{(\Delta h)}(q,u)\,T_{\mu\nu}(q,u),
\end{aligned}
\tag{8}
$$

in terms of a complete set of Lorentz structures $L_{\mu\nu}^{(ij)}(q,u)$ and $T_{\mu\nu}(q,u)$. A convenient basis that enjoys projector properties

was suggested in [20]. We recall the definitions

$$\begin{aligned} L^{(22)}_{\mu\nu}(q,u) &= \left[\frac{(q\cdot u)}{q^2}\,q_\mu - u_\mu\right]\frac{q^2}{q^2-(q\cdot u)^2} \\ &\quad\times\left[\frac{(q\cdot u)}{q^2}\,q_\nu - u_\nu\right], \\ L^{(12)}_{\mu\nu}(q,u) &= L^{(21)}_{\nu\mu}(q,u) = q_\mu\sqrt{\frac{1}{q^2-(q\cdot u)^2}} \\ &\quad\times\left[\frac{(q\cdot u)}{q^2}\,q_\nu - u_\nu\right], \\ L^{(11)}_{\mu\nu}(q,u) &= \frac{q_\mu\,q_\nu}{q^2}, \\ T_{\mu\nu}(q,u) &= g_{\mu\nu} - \frac{q_\mu\,q_\nu}{q^2} - L^{(22)}_{\mu\nu}(q,u). \end{aligned} \tag{9}$$

The presentation of explicit expressions for the longitudinal and transverse nucleon- and isobar-hole loop functions is relegated to Appendix A. The latter follow by a simple contraction of the tensors $\Pi_{\mu\nu}(q,u)$ with the projectors in Eq. (9). The results depend on the details of the in-medium isobar propagator which will be specified in Secs. V and VI.

Following [20] we construct the pion self-energy in terms of the longitudinal nucleon- and isobar-hole loop functions. The self-energy can be cast into the form of a sum of 11, 33 and 13, 31 components of an appropriate 4×4 matrix,

$$\begin{aligned} \Pi(q,u) = -4\,\pi\left(1+\frac{m_\pi}{m_N}\right) b_{\rm eff}\,\rho \\ - q^2\,[(1-\Pi^{(L)}\,g^{(L)})^{-1}\,\Pi^{(L)}]_{11} \\ - q^2\,[(1-\Pi^{(L)}\,g^{(L)})^{-1}\,\Pi^{(L)}]_{33} \\ - q^2\,[(1-\Pi^{(L)}\,g^{(L)})^{-1}\,\Pi^{(L)}]_{13} \\ - q^2\,[(1-\Pi^{(L)}\,g^{(L)})^{-1}\,\Pi^{(L)}]_{31}, \end{aligned} \tag{10}$$

where

$$\begin{aligned} g^{(L)} &= \begin{pmatrix} g'_{11} & 0 & g'_{12} & 0 \\ 0 & g'_{11} & 0 & g'_{12} \\ g'_{12} & 0 & g'_{22} & 0 \\ 0 & g'_{12} & 0 & g'_{22} \end{pmatrix}, \\ \Pi^{(L)} &= \begin{pmatrix} \Pi^{(Nh)}_{11} & \Pi^{(Nh)}_{12} & 0 & 0 \\ \Pi^{(Nh)}_{21} & \Pi^{(Nh)}_{22} & 0 & 0 \\ 0 & 0 & \Pi^{(\Delta h)}_{11} & \Pi^{(\Delta h)}_{12} \\ 0 & 0 & \Pi^{(\Delta h)}_{21} & \Pi^{(\Delta h)}_{22} \end{pmatrix}. \end{aligned} \tag{11}$$

In Eq. (10) we allow for a background term linear in the nuclear density reflecting a s-wave pion-nucleon interaction. Such a term is motivated by the fact that the vertices of Eq. (1) do not reproduce the empirical s-wave scattering pion-nucleon length. At tree-level the vertices (1) lead to a pion-nucleon isospin averaged scattering length of the form [26]

$$4\,\pi\left(1+\frac{m_\pi}{m_N}\right) a_{\pi N} = -\frac{f_N^2}{m_N} - \frac{8}{9}\,\frac{f_\Delta^2}{m_\Delta}\left(1+2\,\frac{m_N}{2\,m_\Delta}\right). \tag{12}$$

This leads to $a_{\pi N}\simeq -0.09$ fm, a significant overestimation of the empirical scattering length of about -0.01 fm [26]. Using the unitarized isobar propagator as implied by the one-loop isobar self-energy of Sec. V we obtain $a_{\pi N}\simeq +0.00$ fm instead, a value significantly reduced and closer to the empirical constraint. In order to correct for the remaining slight mismatch we use $b_{\rm eff}\simeq -0.01$ fm in Eq. (10). We note that the model (8) neglects two-particle two-hole contributions that can not be associated with the in-medium width of the isobar. Given an empirical total absorption strength the size of the latter will depend crucially on the detailed results claimed for the in-medium properties of the isobar.

There are two important technical issues we need to emphasize here. First the application of the longitudinal and transverse projectors in Eq. (8) implies that the loop functions have to satisfy specific constraint conditions. They follow from the observation that the polarization tensor $\Pi_{\mu\nu}(q,u)$ is regular, in particular at $q^2=0$ and at $q^2=(q\cdot u)^2$. Confronting the decomposition (8) with the limiting expressions of (9) for $q^2\to 0$ and $q^2-(q\cdot u)^2\to 0$ establishes the relations

$$\begin{aligned} &\Pi_{22}(q,u) = \Pi_{11}(q,u) - i\,\Pi_{12}(q,u) - i\,\Pi_{21}(q,u) + \mathcal{O}(q^2), \\ &\Pi_{22}(q,u) = \Pi_T(q,u) + \mathcal{O}((q\cdot u)^2 - q^2). \end{aligned} \tag{13}$$

The reader may wonder why we discuss this point. After all the integrals (7) are finite and the conditions (13) should be satisfied automatically. However, we argue in favor of a finite renormalization which is not necessarily compatible with Eq. (13). A finite renormalization of the isobar-hole loop functions is useful as to suppress the formation of ghosts in the pion self-energy. The latter may be absorbed into a redefinition of the Migdal's short-range interaction (2). The occurrence of ghost causes a severe problem, in particular in a self-consistent approach. It implied that the pion self-energy does not satisfy a Lehman representation anymore. A ghost state is present if the pion self-energy has a pole for complex energies, i.e.,

$$D(\omega) = \det[1-\Pi^{(L)}(\omega,\vec{q}\,)\,g^L] = 0 \quad \text{with} \quad \Im\omega\neq 0. \tag{14}$$

Note that a function that satisfies a Lehman representation can have poles only on the second or higher Riemann sheets. In fact, we observe that such artifacts are avoided typically once a finite renormalization is implemented such that all elements $\Pi_{ij}(\omega,\vec{q}\,)$ are bounded for large energies, i.e.,

$$\lim_{\omega\to\pm\infty}|\Pi_{ij}(\omega,\vec{q}\,)| < \infty. \tag{15}$$

As detailed in Appendix A we introduce a finite renormalization for the isobar-hole loop functions by insisting on subtracted dispersion-integral representations thereof. The construction of the latter was determined by the constraints (13). We checked that our numerical pion self-energies satisfy a once-subtracted dispersion-integral representation to reasonable accuracy. In our self-consistent simulations we

impose such a dispersion-integral representation, where the subtraction constant is determined as to find agreement with the direct computation at $\omega^2 - \vec{q}^{\,2} = m_\pi^2$.

It is evident that there is a self-consistency issue here. The isobar propagator defining the isobar-hole loop functions in Eq. (7) is a crucial ingredient to evaluate the pion self-energy. Since, the isobar self-energy depends sensitively on the pion propagator itself a self-consistent computation is required. The importance of self-consistency, as discussed above, will be addressed in the second to last section when presenting numerical results.

IV. ISOBAR PROPAGATOR

The solution of the Dyson equation (6) requires a detailed study of the Lorentz-Dirac structure of the isobar propagator. Consider the propagator, $S_{\mu\nu}(w,u)$, in the nuclear medium. From covariance we expect a general decomposition of the form

$$S^{\mu\nu}(w,u) = \sum_{i,j} S^{(p)}_{[ij]}(v,u)\, P^{\mu\nu}_{[ij]}(v,u) + \sum_{i,j} S^{(q)}_{[ij]}(v,u)\, Q^{\mu\nu}_{[ij]}(v,u), \tag{16}$$

in terms of invariant functions, $S^{(p,q)}_{[ij]}(v,u)$, and a complete set of Dirac-Lorentz tensors $P^{\mu\nu}_{[ij]}(v,u)$ and $Q^{\mu\nu}_{[ij]}(v,u)$. For latter convenience we introduce

$$v_\mu = w_\mu - \Sigma^N_V\, u_\mu. \tag{17}$$

A suitable basis was constructed in [26,27], enjoying the projector properties

$$\begin{aligned} Q^{\mu\alpha}_{[ik]}\, g_{\alpha\beta}\, P^{\beta\nu}_{[lj]} &= 0 = P^{\mu\alpha}_{[ik]}\, g_{\alpha\beta}\, Q^{\beta\nu}_{[lj]},\\ Q^{\mu\alpha}_{[ik]}\, g_{\alpha\beta}\, Q^{\beta\nu}_{[lj]} &= \delta_{kl}\, Q^{\mu\nu}_{[ij]},\\ P^{\mu\alpha}_{[ik]}\, g_{\alpha\beta}\, P^{\beta\nu}_{[lj]} &= \delta_{kl}\, P^{\mu\nu}_{[ij]}. \end{aligned} \tag{18}$$

This particular basis streamlines the computation of the in-medium part of the isobar self-energy significantly. It was applied also in [24]. In particular the algebra (18) illustrates the decoupling of helicity one-half (p-space) and three-half modes (q-space). Decomposing the isobar self-energy

$$\Sigma^{\mu\nu}(w,u) = \sum_{i,j} \Sigma^{(p)}_{[ij]}(v,u)\, P^{\mu\nu}_{[ij]}(v,u) + \sum_{i,j} \Sigma^{(q)}_{[ij]}(v,u)\, Q^{\mu\nu}_{[ij]}(v,u), \tag{19}$$

into the set of projectors it is straightforward to evaluate the isobar propagator. The Dyson equation (6) maps onto two simple matrix equations. First, the bare propagator

$$S^{\mu\nu}_0(w) = \sum_{i,j} S^{(p)}_{0,[ij]}(v,u)\, P^{\mu\nu}_{[ij]}(v,u) + \sum_{i,j} S^{(q)}_{0,[ij]}(v,u)\, Q^{\mu\nu}_{[ij]}(v,u), \tag{20}$$

needs to be decomposed in terms of the projectors. Second, the six-dimensional matrix $\Sigma^{(p)}(v,u)$ and two-dimensional matrix $\Sigma^{(q)}(v,u)$ have to be evaluated. The final form of the isobar propagator, specified in terms of the invariant matrices $S^{(p)}(v,u)$ and $S^{(q)}(v,u)$, follows by simple matrix manipulations:

$$\begin{aligned} S^{(p)}(v,u) &= S^{(p)}_0(v,u)\left[1 - \Sigma^{(p)}(v,u)\, S^{(p)}_0(v,u)\right]^{-1},\\ S^{(q)}(v,u) &= S^{(q)}_0(v,u)\left[1 - \Sigma^{(q)}(v,u)\, S^{(q)}_0(v,u)\right]^{-1}. \end{aligned} \tag{21}$$

The transparent expressions (21) rely on the explicit availability of the projector algebra. In order to keep this work self-contained we review briefly the set of projectors $P^{\mu\nu}_{[ij]}(v,u)$ and $Q^{\mu\nu}_{[ij]}(v,u)$ introduced in [27]. It is convenient to express the latter in terms of appropriate building blocks $P_\pm, U_\pm, V_\mu$ and L_μ, R_μ of the form

$$\begin{aligned} P_\pm(v) &= \frac{1}{2}\left(1 \pm \frac{\not{v}}{\sqrt{v^2}}\right),\\ U_\pm(v,u) &= P_\pm(v)\, \frac{-i\,\gamma\cdot u}{\sqrt{(v\cdot u)^2/v^2 - 1}}\, P_\mp(v),\\ V_\mu(v) &= \frac{1}{\sqrt{3}}\left(\gamma_\mu - \frac{\not{v}}{v^2}\, v_\mu\right),\\ X_\mu(v,u) &= \frac{(v\cdot u)\, v_\mu - v^2\, u_\mu}{v^2\,\sqrt{(v\cdot u)^2/v^2 - 1}},\\ R_\mu(v,u) &= +\frac{1}{\sqrt{2}}\,(U_+(v,u) + U_-(v,u))\, V_\mu(v) - i\,\sqrt{\frac{3}{2}}\, X_\mu(v,u),\\ L_\mu(v,u) &= +\frac{1}{\sqrt{2}}\, V_\mu(v)(U_+(v,u) + U_-(v,u)) - i\,\sqrt{\frac{3}{2}}\, X_\mu(v,u). \end{aligned} \tag{22}$$

For a compilation of useful properties of the building blocks $P_\pm, U_\pm, V_\mu$ and R_μ, L_μ we refer to the original work [27]. The q-space projectors are

$$\begin{aligned} Q^{\mu\nu}_{[11]} &= (g^{\mu\nu} - \hat{v}^\mu\,\hat{v}^\nu)\, P_+ - V^\mu\, P_-\, V^\nu - L^\mu\, P_+\, R^\nu,\\ Q^{\mu\nu}_{[22]} &= (g^{\mu\nu} - \hat{v}^\mu\,\hat{v}^\nu)\, P_- - V^\mu\, P_+\, V^\nu - L^\mu\, P_-\, R^\nu,\\ Q^{\mu\nu}_{[12]} &= (g^{\mu\nu} - \hat{v}^\mu\,\hat{v}^\nu)\, U_+ + \tfrac{1}{3}\, V^\mu\, U_-\, V^\nu + \tfrac{\sqrt{8}}{3}\,(L^\mu\, P_+\, V^\nu + V^\mu\, P_-\, R^\nu) - \tfrac{1}{3}\, L^\mu\, U_+\, R^\nu,\\ Q^{\mu\nu}_{[21]} &= (g^{\mu\nu} - \hat{v}^\mu\,\hat{v}^\nu)\, U_- + \tfrac{1}{3}\, V^\mu\, U_+\, V^\nu + \tfrac{\sqrt{8}}{3}\,(L^\mu\, P_-\, V^\nu + V^\mu\, P_+\, R^\nu) - \tfrac{1}{3}\, L^\mu\, U_-\, R^\nu, \end{aligned} \tag{23}$$

where $\hat{v}_\mu = v_\mu/\sqrt{v^2}$. It is straightforward to verify Eq. (18). Using the properties of the building blocks $P_\pm, U_\pm, V_\mu$ and L_μ, R_μ [27] reveals that the objects $Q^{\mu\nu}_{[ij]}$ indeed form a projector algebra.

The p-space projectors have similar transparent representations. Following [27] it is convenient to extend the p-space algebra including objects with one or no Lorentz index,

$$
\begin{aligned}
&P_{[11]} = P_+, && P_{[12]} = U_+, && P_{[21]} = U_-, && P_{[22]} = P_-,\\
&P^\mu_{[31]} = V^\mu\, P_+, && P^\mu_{[32]} = V^\mu\, U_+, && \bar P^\mu_{[13]} = P_+\, V^\mu, && \bar P^\mu_{[23]} = U_-\, V^\mu,\\
&P^\mu_{[41]} = V^\mu\, U_-, && P^\mu_{[42]} = V^\mu\, P_-, && \bar P^\mu_{[14]} = U_+\, V^\mu, && \bar P^\mu_{[24]} = P_-\, V^\mu,\\
&P^\mu_{[51]} = \hat v^\mu\, P_+, && P^\mu_{[52]} = \hat v^\mu\, U_+, && \bar P^\mu_{[15]} = P_+\, \hat v^\mu, && \bar P^\mu_{[25]} = U_-\, \hat v^\mu,\\
&P^\mu_{[61]} = \hat v^\mu\, U_-, && P^\mu_{[62]} = \hat v^\mu\, P_-, && \bar P^\mu_{[16]} = U_+\, \hat v^\mu, && \bar P^\mu_{[26]} = P_-\, \hat v^\mu,\\
&P^\mu_{[71]} = L^\mu\, P_+, && P^\mu_{[72]} = L^\mu\, U_+, && \bar P^\mu_{[17]} = P_+ R^\mu, && \bar P^\mu_{[27]} = U_- R^\mu,\\
&P^\mu_{[81]} = L^\mu\, U_-, && P^\mu_{[82]} = L^\mu\, P_-, && \bar P^\mu_{[18]} = U_+ R^\mu, && \bar P^\mu_{[28]} = P_- R^\mu,
\end{aligned}
$$

$$
P^{\mu\nu}_{[i\,j]} = P^\mu_{[i1]}\, \bar P^\nu_{[1\,j]} = P^\mu_{[i2]}\, \bar P^\nu_{[2\,j]}. \tag{24}
$$

In the notation of Eq. (25) the indices i, j in Eqs. (16), (19), (20) run from 3 to 8 in the p-space. The set of identities (18) extends naturally

$$
\begin{aligned}
&P_{[ik]}\cdot P_{[lj]} = \delta_{kl}\, P_{[ij]}, \quad P^\mu_{[ik]}\, \bar P^\nu_{[lj]} = \delta_{kl}\, P^{\mu\nu}_{[ij]},\\
&\bar P^\mu_{[ik]}\, g_{\mu\nu}\, P^\nu_{[lj]} = \delta_{kl}\, P_{[ij]},\\
&Q^{\mu\alpha}_{[ik]}\, g_{\alpha\beta}\, P^\beta_{[lj]} = 0 = \bar P^\alpha_{[ik]}\, g_{\alpha\beta}\, Q^{\beta\nu}_{[lj]}.
\end{aligned} \tag{25}
$$

The algebra (25) proves convenient in solving various problems. Using the projector formalism we compute the in-medium isobar self-energy as implied by the interaction vertex (1) at the one-loop level in a manifest covariant fashion.

V. ISOBAR SELF-ENERGY AND PION-NUCLEON SCATTERING

It proves convenient to extract the isobar propagator from an appropriately constructed model of the pion-nucleon scattering amplitude. Set up in this way all results are induced by expressions already presented in [27] upon the application of simple substitution rules. Recall the in-medium Bethe-Salpeter equation,

$$
\begin{aligned}
\mathcal{T}(\bar k, k; w, u) &= \mathcal{V}(\bar k, k; w, u) + \int \frac{d^4 l}{(2\pi)^4}\, \mathcal{V}(\bar k, l; w, u)\\
&\quad \times \mathcal{G}(l; w, u)\, \mathcal{T}(l, k; w, u),
\end{aligned} \tag{26}
$$

$$
\mathcal{G}\left(\frac{1}{2}\, w - l; w, u\right) = -i\, S(w - l, u)\left[l^2 - m_\pi^2 - \Pi(l, u)\right]^{-1},
$$

where $q, p, \bar q, \bar p$ are the initial and final pion and nucleon four-momenta and

$$
w = p + q = \bar p + \bar q, \quad k = \tfrac{1}{2}\,(p - q), \quad \bar k = \tfrac{1}{2}\,(\bar p - \bar q). \tag{27}
$$

The two-particle propagator, $\mathcal{G}(l; w, u)$, is specified in terms of the nucleon propagator $S(p, u)$ of Eq. (3) and the pion propagator written in terms of the in-medium self energy $\Pi(l, u)$ of Eq. (10).

In order to generate the isobar self-energy $\Sigma^{\mu\nu}(w, u)$, we introduce the interaction kernel

$$
\mathcal{V}(\bar k, k; w, u) = -\frac{f_\Delta^2}{m_\pi^2}\, \bar q_\mu\, S_0^{\mu\nu}\big(w - \Sigma_V^\Delta\, u\big)\, q_\nu, \tag{28}
$$

where we allow for the presence of a vector mean field. The isospin projector is suppressed in Eq. (28) (see, e.g., [21]). The particular choice (28) implies a scattering amplitude, which determines the isobar propagator, $S_{\mu\nu}(w, u)$, by

$$
\mathcal{T}(\bar k, k; w, u) = -\frac{f_\Delta^2}{m_\pi^2}\, \bar q_\mu\, S^{\mu\nu}(w, u)\, q_\nu. \tag{29}
$$

The system is solved conveniently by decomposing the interaction kernel into a set of projectors, where we apply the projectors constructed in terms of the four-momentum $v_\mu = w_\mu - \Sigma_V\, u_\mu$ and u_μ rather than w_μ and u_μ:

$$
\begin{aligned}
\mathcal{V} = &\sum_{i,j} V^{(p)}_{[ij]}(v, u)\, \bar q_\mu\, P^{\mu\nu}_{[ij]}(v, u)\, q_\nu\\
&+ \sum_{i,j} V^{(q)}_{[ij]}(v, u)\, \bar q_\mu\, Q^{\mu\nu}_{[ij]}(v, u)\, q_\nu.
\end{aligned} \tag{30}
$$

For the general case with $\Sigma_V^\Delta \neq \Sigma_V^N$ the derivation of $V^{(p,q)}_{[ij]}(v, u)$ as implied by Eq. (28) is somewhat tedious though straight forward. The expressions are listed in Appendix B. In the limit $\Sigma_V^\Delta \to \Sigma_V^N$ the expressions simplify with

$$
\begin{aligned}
V^{(q)}_{[11]} &= V^{(p)}_{[77]} = +\frac{f_\Delta^2}{m_\pi^2}\, \frac{1}{\sqrt{v^2} - m_\Delta},\\
V^{(q)}_{[22]} &= V^{(p)}_{[88]} = -\frac{f_\Delta^2}{m_\pi^2}\, \frac{1}{\sqrt{v^2} + m_\Delta},\\
V^{(p)}_{[55]} &= -\frac{2}{3}\, \frac{f_\Delta^2}{m_\pi^2}\, \frac{\sqrt{v^2} + m_\Delta}{m_\Delta^2},\\
V^{(p)}_{[66]} &= +\frac{2}{3}\, \frac{f_\Delta^2}{m_\pi^2}\, \frac{\sqrt{v^2} - m_\Delta}{m_\Delta^2},
\end{aligned}
$$

$$V^{(p)}_{[53]} = V^{(p)}_{[35]} = +\frac{1}{\sqrt{3}}\,\frac{f^2_\Delta}{m^2_\pi}\,\frac{1}{m_\Delta},$$
$$V^{(p)}_{[64]} = V^{(p)}_{[46]} = -\frac{1}{\sqrt{3}}\,\frac{f^2_\Delta}{m^2_\pi}\,\frac{1}{m_\Delta}, \tag{31}$$

where only components that are nonzero are specified in Eq. (31). A corresponding decomposition is implied for the in-medium scattering amplitude

$$\mathcal{T} = \sum_{i,j} T^{(p)}_{[ij]}(v,u)\,\bar{q}_\mu\,P^{\mu\nu}_{[ij]}(v,u)\,q_\nu + \sum_{i,j} T^{(q)}_{[ij]}(v,u)\,\bar{q}_\mu\,Q^{\mu\nu}_{[ij]}(v,u)\,q_\nu,$$
$$T^{(p)}(v,u) = V^{(p)}(v,u)\,[1 - J^{(p)}(v,u)\,V^{(p)}(v,u)]^{-1},$$
$$T^{(q)}(v,u) = V^{(q)}(v,u)\,[1 - J^{(q)}(v,u)\,V^{(q)}(v,u)]^{-1}. \tag{32}$$

The scattering amplitude $\mathcal{T}$ is determined by the interaction kernel (31) and two matrices of loop functions $J^{(p)}_{[ij]}(v,u)$ and $J^{(q)}_{[ij]}(v,u)$. Comparing Eq. (32) with Eqs. (28) and (21) we identify

$$S^{(p)}_{0,[ij]}(v,u) = -\frac{m^2_\pi}{f^2_\Delta}\,V^{(p)}_{[ij]}(v,u),$$
$$S^{(q)}_{0,[ij]}(v,u) = -\frac{m^2_\pi}{f^2_\Delta}\,V^{(q)}_{[ij]}(v,u),$$
$$\Sigma^{(p)}_{[ij]}(v,u) = -\frac{f^2_\Delta}{m^2_\pi}\,J^{(p)}_{[ij]}(v,u),$$
$$\Sigma^{(q)}_{[ij]}(v,u) = -\frac{f^2_\Delta}{m^2_\pi}\,J^{(q)}_{[ij]}(v,u). \tag{33}$$

The form of the loop functions can be taken over from [27,28]. The evaluation of the real parts of the loop functions requires great care. The imaginary parts of the loop functions are unbounded at large energies. Thus power divergencies arise if the real parts are evaluated by means of an unsubtracted dispersion-integral ansatz. The task is to device a subtraction scheme that avoids kinematical singularities and that eliminates all power divergent terms systematically. The latter are unphysical and in a consistent effective field theory approach must be absorbed into counter terms. Only the residual strength of the counter terms may be estimated by a naturalness assumption reliably. Since we want to neglect such counter terms it is crucial to set up the renormalization in a proper manner. The scheme developed in [28] avoids the occurrence of power-divergent structures and is free of kinematical singularities.

The loop functions $J^{(p,q)}_{[ij]}(v_0\,,\vec{w}\,)$ are expressed in terms of a basis spanned by 13 master loop functions, $J_n(v_0\,,\vec{w}\,)$ as detailed in [28]. We assume nuclear matter at rest for simplicity. The master loop functions are evaluated by a dispersion integral of the form

$$J_n(v_0,\vec{w}\,) = \int_{-\infty}^{+\infty}\frac{d\bar{v}_0}{\pi}\,\frac{\Delta J_n(\bar{v}_0;v_0,\vec{w}\,)}{\bar{v}_0 - v_0 - i\,\epsilon\,(\bar{v}_0-\mu)} \times \mathrm{sign}\,(\bar{v}_0-\mu) + J^C_n(v_0,\vec{w}\,), \tag{34}$$

where $\mu^2 = m^2_N + k^2_F$. We introduce spectral weight functions, $\Delta J_n(\bar{v}_0;v_0,\vec{w}\,)$, that depend on 'external' and 'internal' energies $v_0 = w_0 - \Sigma_V$ and $\bar{v}_0$. We identify

$$\Delta J_n(\bar{v}_0;v_0,\vec{w}) = \int\frac{d^3l}{2\,(2\pi)^3}\,\left(m^2_N + \vec{l}^{\,2}\right)^{-\frac{1}{2}} \times\Big\{K^R_n(l_+,\bar{v}_0;v_0,\vec{w}\,)\,\rho_\pi(|\bar{v}_+|,\vec{w}-\vec{l}) \times[\Theta(+\bar{v}_+) - \Theta(k_F - |\vec{l}\,|)] + K^R_n(l_-,\bar{v}_0;v_0,\vec{w}\,) \times\rho_\pi(|\bar{v}_-|,\vec{w}-\vec{l}\,)\,\Theta(-\bar{v}_-)\Big\},$$
$$l^\mu_\pm = \left(\pm\sqrt{m^2_N + \vec{l}^{\,2}},\vec{l}\right), \qquad \bar{v}_\pm = \bar{v}_0 \mp \sqrt{m^2_N + \vec{l}^{\,2}}, \tag{35}$$

where the explicit form of the kernels K^R_n as well as of the counter loops $J^C_n(v_0,\vec{w})$ are recalled in [28]. The kernels are invariant functions of the four-vectors l_μ, v_μ, $\bar{v}_\mu$ and u_μ. The spectral density of the pion, $\rho_\pi(\omega,\vec{q}\,)$, is

$$\rho_\pi(\omega,\vec{q}\,) = -\Im\,\frac{1}{\omega^2 - \vec{q}^{\,2} - m^2_\pi - \Pi(\omega,\vec{q}\,)}. \tag{36}$$

VI. ISOBAR SELF-ENERGY IN THE PRESENCE OF VERTEX CORRECTIONS

The evaluation of the loop functions in the presence of vertex corrections is particularly challenging due to their complicated ultraviolet behavior. In Fig. 3 the two types of contributions are depicted graphically in terms of vertex functions to be specified below. It is useful to identify a set of master loop functions, in terms of which the full loop matrix can be constructed. The latter are renormalized applying the scheme introduced in the previous section. The proper generalization of Eq. (35) is readily worked out. The pion spectral function is distorted by vertex correction functions

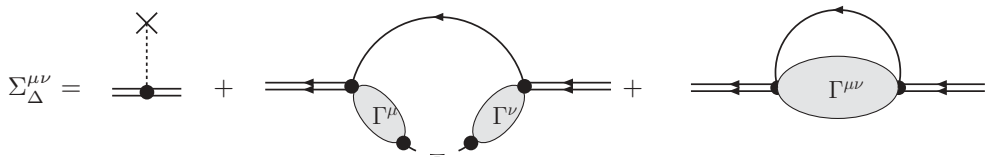

FIG. 3. Isobar self-energy in the presence of short-range correlations. The solid line shows a nucleon propagator in the presence of mean fields. The dashed line represents a dressed pion propagator.

leading to effective spectral densities, which we denote with $\rho_{ab}(\omega,\vec{q}\,)$. For a given spectral distribution we introduce

$$\begin{aligned}\Delta J_{ab,n}(\bar v_0;v_0,\vec w) &= \int \frac{d^3l}{2(2\pi)^3}\,\big(m_N^2+\vec l^{\,2}\big)^{-\frac12}\\ &\times\Bigg\{K_n(l_+,\bar v_0;v_0,\vec w)\,\rho_{ab}(|\bar v_+|,\vec w-\vec l\,)\\ &\times\left[\Theta(+\bar v_+)-\left(\frac{\bar v_+}{|\bar v_+|}\right)^{a+b}\Theta(k_F-|\vec l\,|)\right]\\ &+\left(\frac{\bar v_-}{|\bar v_-|}\right)^{a+b}K_n(l_-,\bar v_0;v_0,\vec w)\\ &\times\rho_{ab}(|\bar v_-|,\vec w-\vec l\,)\,\Theta(-\bar v_-)\Bigg\},\\ l_\pm^\mu &= \big(\pm\sqrt{m_N^2+\vec l^{\,2}},\vec l\big),\\ \bar v_\pm &= \bar v_0\mp\sqrt{m_N^2+\vec l^{\,2}},\end{aligned}\tag{37}$$

where $n=0,\ldots,12$. The kernels $K_n(l,\bar v_0;v_0,\vec w)$ are identical to those encountered in Eq. (35). They are listed in [28]. The real part of the loop functions is computed applying the dispersion-integral representation (34). A corresponding generalization holds for the second term in Eq. (34).

We identify the effective spectral distributions, $\rho_{ab}(\omega,\vec{q}\,)$ as implied by the diagrams of Fig. 3. The vertex vector and tensor may be decomposed into invariants

$$\begin{aligned}\Gamma^\mu(q,u) &= q^\mu\,\Gamma_1(q,u)+u^\mu\,\Gamma_2(q,u),\\ \Gamma^{\mu\nu}(q,u) &= q^\mu q^\nu\Gamma_{11}(q,u)+q^\mu u^\nu\,\Gamma_{12}(q,u)\\ &\quad+u^\mu q^\nu\,\Gamma_{12}(q,u)+u^\mu u^\nu\,\Gamma_{22}(q,u)\\ &\quad+g^{\mu\nu}\,\Gamma_{00}(q,u),\end{aligned}\tag{38}$$

in terms of which we introduce the spectral distributions

$$\begin{aligned}\rho_{00}(\omega,\vec q\,) &= -\Im\,(\Gamma_{00}(\omega,\vec q\,)),\\ \rho_{ab}(\omega,\vec q\,) &= -\Im\left(\frac{\Gamma_a(\omega,\vec q\,)\,\Gamma_b(\omega,\vec q\,)}{\omega^2-\vec q^{\,2}-m_\pi^2-\Pi_\pi(\omega,\vec q\,)}+\Gamma_{ab}(\omega,\vec q\,)\right).\end{aligned}\tag{39}$$

Applying the techniques introduced in [20] it is straightforward to express $\Gamma_1(q,u)$ and $\Gamma_2(q,u)$ in terms of the longitudinal coupling matrix, $g^{(L)}$, and the loop functions, $\Pi^{(L)}(q,u)$ of Eqs. (8), (11). We obtain

$$\begin{aligned}\Gamma_1(q,u) &= [1-g^{(L)}\,\Pi^{(L)}(q,u)]^{-1}_{31}+[1-g^{(L)}\,\Pi^{(L)}(q,u)]^{-1}_{33}\\ &\quad+\frac{q\cdot u}{\sqrt{q^2-(q\cdot u)^2}}\big([1-g^{(L)}\,\Pi^{(L)}(q,u)]^{-1}_{41}\\ &\quad+[1-g^{(L)}\,\Pi^{(L)}(q,u)]^{-1}_{43}\big),\\ \Gamma_2(q,u) &= -\frac{q^2}{\sqrt{q^2-(q\cdot u)^2}}\big([1-g^{(L)}\,\Pi^{(L)}(q,u)]^{-1}_{41}\\ &\quad+[1-g^{(L)}\,\Pi^{(L)}(q,u)]^{-1}_{43}\big).\end{aligned}\tag{40}$$

The matrix $\Gamma_{ab}(q,u)$ probes longitudinal and transverse correlations. As an extension of Eq. (11) we introduce a transverse coupling and loop matrix $g^{(T)}$ and $\Pi^{(T)}(q,u)$. We write

$$\begin{aligned}g^{(T)} &= \begin{pmatrix} g'_{11} & g'_{12}\\ g'_{21} & g'_{22}\end{pmatrix},\\ \Pi^{(T)}(q,u) &= \begin{pmatrix}\Pi_T^{(Nh)}(q,u) & 0\\ 0 & \Pi_T^{(\Delta h)}(q,u)\end{pmatrix}.\end{aligned}\tag{41}$$

We derive explicit forms of the tensor vertex

$$\begin{aligned}\Gamma_{11}(q,u) &= \frac{1}{q^2}\left(\chi_{33}^{(L)}+\frac{q\cdot u}{\sqrt{q^2-(q\cdot u)^2}}\big(\chi_{34}^{(L)}+\chi_{43}^{(L)}\big)\right.\\ &\quad\left.+\frac{(q\cdot u)^2}{q^2-(q\cdot u)^2}\,\chi_{44}^{(L)}-\frac{q^2}{q^2-(q\cdot u)^2}\,\chi_{22}^{(T)}\right),\\ \Gamma_{12}(q,u) &= \Gamma_{21}(q,u)=-\frac{1}{\sqrt{q^2-(q\cdot u)^2}}\,\chi_{34}^{(L)}\\ &\quad-\frac{q\cdot u}{q^2-(q\cdot u)^2}\big(\chi_{44}^{(L)}-\chi_{22}^{(T)}\big),\\ \Gamma_{22}(q,u) &= \frac{q^2}{q^2-(q\cdot u)^2}\big(\chi_{44}^{(L)}-\chi_{22}^{(T)}\big),\\ \Gamma_{00}(q,u) &= \chi_{22}^{(T)},\end{aligned}\tag{42}$$

in terms of the longitudinal and transverse correlation functions

$$\chi^{(L,T)}(q,u)=[1-g^{(L,T)}\,\Pi^{(L,T)}(q,u)]^{-1}\,g^{(L,T)}.\tag{43}$$

In the course of deriving the representation (37) we made use of the following properties of the correlation functions:

$$\begin{aligned}\Pi_{ij}^{(L)}(-\omega,\vec q\,) &= (-1)^{i+j}\,\Pi_{ij}^{(L)}(+\omega,\vec q\,),\\ \Pi_{ij}^{(T)}(-\omega,\vec q\,) &= (-1)^{i+j}\,\Pi_{ij}^{(T)}(+\omega,\vec q\,),\\ \Gamma_a(-\omega,\vec q\,) &= (-1)^{a+1}\,\Gamma_a(+\omega,\vec q\,),\\ \Gamma_{ab}(-\omega,\vec q\,) &= (-1)^{a+b}\,\Gamma_{ab}(+\omega,\vec q\,).\end{aligned}\tag{44}$$

It is left to specify the isobar self-energy in terms of the generic loop functions defined by Eq. (37). In a first step a matrix of loop functions, $J^{(p,q)}_{ab,[ij]}(v,u)$, is constructed in terms of $J_{ab,n}(v,u)$ as detailed in [28]. The latter correspond to the projector algebra of Sec. IV. The evaluation of the self-energy is analogous to the computation of Sec. IV with the slight complication that the effective vertex develops additional structures $q_\mu u_\mu+u_\mu q_\nu, u_\mu u_\nu$, and $g_{\mu\nu}$. The loops $J^{(p,q)}_{11,[ij]}(v,u)$, which are implied by the structure $q_\mu q_\nu$, contribute like the previous loops $J^{(p,q)}_{[ij]}(v,u)$ in Eq. (33). The implication of the remaining loop functions is readily worked out upon the application of the useful identities

$$\begin{aligned}u^\mu &= -i\sqrt{\frac23}\sqrt{\frac{(v\cdot u)^2}{v^2}-1}\left\{\bar P^\mu_{[17]}+\bar P^\mu_{[28]}\right.\\ &\quad\left.-\frac{1}{\sqrt2}\big(\bar P^\mu_{[14]}+\bar P^\mu_{[23]}\big)\right\}+\frac{v\cdot u}{\sqrt{v^2}}\big(\bar P^\mu_{[15]}+\bar P^\mu_{[26]}\big)\\ &= -i\sqrt{\frac23}\sqrt{\frac{(v\cdot u)^2}{v^2}-1}\end{aligned}$$

$$\times \left\{ P^{\mu}_{[71]} + P^{\mu}_{[82]} - \frac{1}{\sqrt{2}} \left(P^{\mu}_{[41]} + P^{\mu}_{[32]} \right) \right\}$$
$$+ \frac{v \cdot u}{\sqrt{v^2}} \left(P^{\mu}_{[51]} + P^{\mu}_{[62]} \right),$$
$$g^{\mu\nu} P_{[11]} = Q^{\mu\nu}_{[11]} + P^{\mu\nu}_{[44]} + P^{\mu\nu}_{[55]} + P^{\mu\nu}_{[77]},$$
$$g^{\mu\nu} P_{[22]} = Q^{\mu\nu}_{[22]} + P^{\mu\nu}_{[33]} + P^{\mu\nu}_{[66]} + P^{\mu\nu}_{[88]},$$
$$g^{\mu\nu} P_{[12]} = Q^{\mu\nu}_{[12]} - \frac{1}{3} P^{\mu\nu}_{[43]} + P^{\mu\nu}_{[56]} + \frac{1}{3} P^{\mu\nu}_{[78]}$$
$$- \frac{\sqrt{8}}{3} \left(P^{\mu\nu}_{[73]} + P^{\mu\nu}_{[48]} \right),$$
$$g^{\mu\nu} P_{[21]} = Q^{\mu\nu}_{[21]} - \frac{1}{3} P^{\mu\nu}_{[34]} + P^{\mu\nu}_{[65]} + \frac{1}{3} P^{\mu\nu}_{[87]}$$
$$- \frac{\sqrt{8}}{3} \left(P^{\mu\nu}_{[84]} + P^{\mu\nu}_{[37]} \right). \tag{45}$$

It is now straightforward to write down the self-energies, $\Sigma^{(p,q)}_{[ij]}(v,u)$. It holds

$$\Sigma^{(q)}_{[ij]}(v,u) = -\frac{f^2_\Delta}{m^2_\pi} \left\{ J^{(q)}_{11,[ij]}(v,u) + J^{(p)}_{00,[ij]}(v,u) \right\},$$
$$\Sigma^{(p)}_{[ij]}(v,u) = -\frac{f^2_\Delta}{m^2_\pi} \left\{ J^{(p)}_{11,[ij]}(v,u) \right.$$
$$+ \sum_{a,b=1}^{2} J^{(p)}_{22,[ab]}(v,u)\, c_{ai}(v,u)\, c_{bj}(v,u)$$
$$+ \sum_{a=1}^{2} \left(J^{(p)}_{12,[ia]}(v,u)\, c_{aj}(v,u) \right.$$
$$+ J^{(p)}_{21,[aj]}(v,u)\, c_{ai}(v,u)$$
$$\left. \left. + \sum_{a,b=1}^{2} J^{(p)}_{00,[ab]}(v,u)\, c^{(ab)}_{[ij]}(v,u) \right\},$$
$$c_{aj}(v,u) = \frac{v \cdot u}{\sqrt{v^2}} \delta_{4+a,j} - i \sqrt{\frac{2}{3}} \sqrt{\frac{(v \cdot u)^2}{v^2} - 1} \tag{46}$$
$$\times \left(\delta_{6+a,j} - \frac{1}{\sqrt{2}} \delta_{5-a,j} \right),$$
$$c^{(ab)}_{[ij]}(v,u) = \delta_{a1}\, \delta_{b2} \left(\frac{1}{3} \left(\delta_{i7}\, \delta_{j8} - \delta_{i4}\, \delta_{j3} \right) + \delta_{i5}\, \delta_{j6} \right.$$
$$\left. - \frac{\sqrt{8}}{3} \left(\delta_{i7}\, \delta_{j3} + \delta_{i4}\, \delta_{j8} \right) \right)$$
$$+ \delta_{ab}\, \delta_{ij} \left(\delta_{i,5-a} + \delta_{i,4+a} + \delta_{i,6+a} \right)$$
$$+ \delta_{a2}\, \delta_{b1} \left(\frac{1}{3} \left(\delta_{i8}\, \delta_{j7} - \delta_{i3}\, \delta_{j4} \right) + \delta_{i6}\, \delta_{j5} \right.$$
$$\left. - \frac{\sqrt{8}}{3} \left(\delta_{i3}\, \delta_{j7} + \delta_{i8}\, \delta_{j4} \right) \right).$$

VII. NUMERICAL RESULTS AND DISCUSSIONS

We present and discuss numerical simulations of the pion and isobar spectral distributions at nuclear saturation density with the Fermi momentum $k_F = 270\,\mathrm{MeV}$. The results depend on a number of parameters appearing in the developed covariant and self-consistent approach. These are first of all the scalar and vector mean-field shifts of the delta, Σ^{Δ}_S and Σ^{Δ}_V, as well as the Migdal parameters g'_{11}, g'_{12}, and g'_{22}. One should also consider medium induced changes in the coupling constants f_Δ and f_N, although it is usually assumed that for nuclear densities they do not depart significantly from their vacuum values. The nucleon mean-field parameters Σ^{S}_N and Σ^{S}_V, which model nuclear saturation and binding effects, are also prone to variations in different models. We use the values $\Sigma^{N}_S = 350\,\mathrm{MeV}$ and $\Sigma^{N}_V = 290\,\mathrm{MeV}$ also assumed in [28,29].

As a guide we consider the values of the above parameters used in earlier computations, but having in mind their scheme dependence. We focus on variations around a parameter set which has been shown to lead to a reproduction of the nuclear photo-absorption cross section in the delta excitation region [29]. The latter study builds on the self-consistent approach developed in this work. It is the first work that considers photo-absorption in the presence of short-range correlation effects in the $\gamma\,\pi\,\pi$, $\gamma\,N\,\Delta$, $\gamma\,\pi\,N\,\Delta$, $\pi\,N\,\Delta$, and $\pi\,N\,N$ vertices. Electromagnetic gauge invariance is kept as a consequence of a series of Ward identities obeyed in the computation. In particular the interference of the in-medium s-channel isobar exchange and the t-channel in-medium pion exchange is considered. We refer to the details of that work which provides the following parameter set:

$$\Sigma^{\Delta}_S = -0.25\,\mathrm{GeV}, \quad \Sigma^{\Delta}_V = -0.11\,\mathrm{GeV},$$
$$g'_{11} = 1.0, \quad g'_{12} = 0.4, \quad g'_{22} = 0.4, \tag{47}$$

together with an in-medium reduction of the f_Δ coupling by 15% but an unchanged value for f_N. According to [2] the in-medium reduction of the f_N coupling is quite small (less than 6% at saturation density). This is in line with our finding that the photo-absorption data does not require any in-medium change of f_N. The values of the Migdal parameters in Eq. (47) are within range of the various sets used in the literature. Though in the recent work by Hees and Rapp [25] large values of g'_{12} and g'_{22} are excluded in their nonrelativistic scheme, this is not the case in our more microscopic and relativistic approach. Values for g'_{12} and g'_{22} as large as in Eq. (47) generate a width for the isobar in [25] that would be incompatible with the photo-absorption data as computed in [25]. However, it is reasonable to expect that such a condition is altered by a possible in-medium reduction of f_Δ. We remark that the significantly different values of nucleon and isobar mean-field self-energies may seem surprising at first, but one should not forget the marked asymmetry in our treatment of the nucleon and the isobar. For the latter we include its self-energy based on the pion-nucleon loop and Migdal's short-range interactions, while for the nucleon the only dressing is through scalar and vector mean fields. An attempt to fit the photo-absorption data assuming similar nucleon and delta mean fields did not yield any useful results.

We recall from [7,29] that the actual position of the photo-absorption peak is a subtle effect of short-range correlation effects and the in-medium isobar properties. The peak of the isobar spectral distribution does not translate directly into the maximum of the photo-absorption cross section. The pion

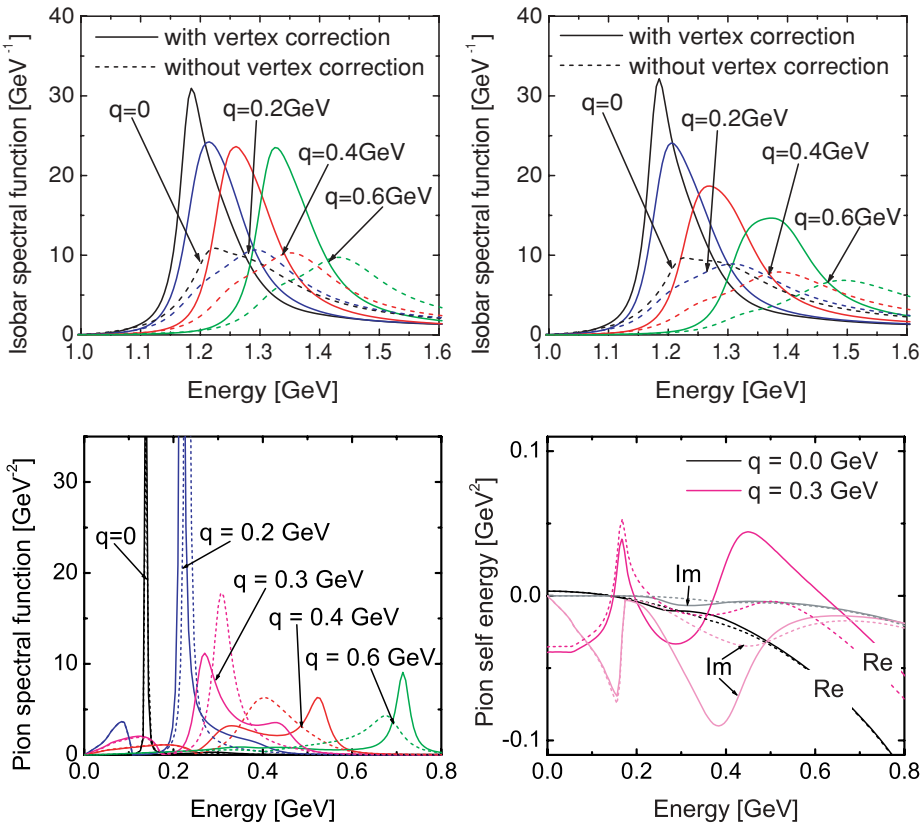

FIG. 4. (Color online) Results for the delta spectral function with (solid lines) and without (dashed lines) the $\pi N \Delta$ vertex correction (upper figures). We show the $S^{(p)}_{[77]}$ component (left figure) and the $S^{(q)}_{[11]}$ component (right figure) for different momenta. The pion spectral function (left figure) and self-energy (right figure) are shown on the lower figures (q is the pion momentum). The parameters of Eq. (47) are used together with our reduced value for f_Δ.

and isobar properties as implied by Eq. (47) are shown in Fig. 4 for nuclear saturation density by solid lines: at zero momentum the isobar receives an attractive mass shift of about 50 MeV. Due to our self-consistent approach this implies that the isobar–nucleon-hole bubble characterizing Migdal's short-range correlations shows structure in an energy region not too dissimilar from the one expected from vacuum masses.

Our predicted mass shift for the isobar is amazingly close to the range obtained in [7] but in stark contrast to the small and repulsive mass shift obtained recently in [25]. For the isobar we restrict the discussion to the two main components because they dominate the resonance region. Please note however, that the proper inclusion of all other components is essential to ensure the cancellation of kinematical singularities on the light-cone.

We observe a significant splitting of the p- and q-space modes at nonzero momentum. The medium effects are stronger for the q-space (helicity 3/2) than they are for the p-space (helicity 1/2), where we obtain a less pronounced broadening and smaller shift in the position of the peak at larger momentum. Note that the nuclear photo-absorption data probe dominantly the helicity 3/2 mode. These findings are in qualitative agreement with the results of [7] that were based on a perturbative and nonrelativistic many-body approach. It should be pointed out, however, that the pion spectral function corresponding to the approach of [7] differs decisively from the one predicted by our approach. Though a direct comparison is difficult, since Oset *et al*. did not provide figures for the pion spectral function, an indirect comparison may be possible. We take the more recent work of Ramos and Oset [34], which provides explicit results for the pion spectral distribution. The strength in the soft pion modes as shown in Fig. 4 is much suppressed as compared to an in-medium pion considered realistic in [34]. Also a comparison of our pion spectral function in Fig. 4 with other recent results [21,22,25] show significant and systematic differences at small and intermediate momenta.

Before we discuss a variation of parameters around the central values (47) we examine the effect of various approximations all based on the parameter set (47). First we consider the effect of neglecting short-range correlation effects in the isobar self-energy as done in [14,21,22]. In Figs. 4 and 5 the quality of such an approximation is scrutinized. Though the Migdal parameters enter in a decisive manner in the computation of the pion self-energy via Eq. (10), the isobar properties are a functional of the pion self-energy and the vertex functions only. As studied in great detail in the previous works [14,21,22], the self-consistent treatment of the pion and isobar properties is an important and significant effect even in the absence of vertex corrections for the isobar. The upper left panel of Fig. 5 shows the contour lines of the pion spectral function as obtained in the fully self-consistent computation. If one neglects the $\pi N \Delta$ vertex correction in the isobar self-energy as discussed above, the contour lines in the upper right-hand panel arise. A more quantitative illustration is offered by a comparison of the solid and dashed lines in Fig. 4. Figures 4 and 5 document the importance of the vertex corrections in the isobar self-energy. Most significant are the effects on the isobar spectral distribution as shown by the solid and dashed lines of Fig. 4. The consistent consideration of

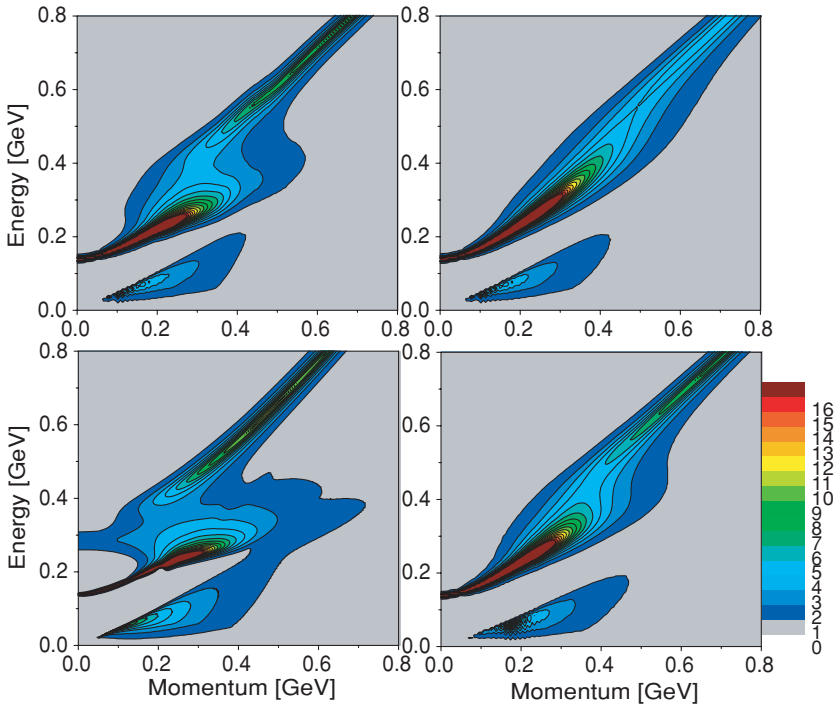

FIG. 5. (Color online) Contour plots of the pion spectral function using the parameters (47). The upper left figure gives our full result, the upper right figure follows if the vertex correction in the delta self-energy are neglected. The lower left figure follows if the free-space isobar propagator is used in Eq. (10). The lower right figure shows the impact of reducing the nucleon mean fields.

short-range correlation effects leads to a significant attractive mass shift and a reduction of the width for the isobar. It is interesting to observe that it appears well justified to treat the vertex contributions in the isobar self-energy in perturbation theory. We find that the evaluation of the vertex bubbles of Fig. 3 with a free-space isobar propagator leads to an isobar propagator that can barely be discriminated from our full results. Recall, however, that a corresponding attempt for the short-range bubbles in the pion self-energy would fail miserably, giving a dramatically different pion spectral function. This is illustrated by the lower left-hand panel of Fig. 5, where the pion spectral function is shown as it is implied by the free-space isobar together with the Migdal parameters of Eq. (47) and our in-medium value for f_Δ. In particular the width of the low-momentum main pion mode would be underestimated.

We now turn to a variation of the parameter set. In the lower right-hand panel Fig. 5 the effect of using smaller scalar and vector mean fields for the nucleons is illustrated. The contour lines were obtained with $\Sigma_S^N = 175$ MeV and $\Sigma_V = 115$ MeV. In Fig. 6 the variation of the value chosen for the $\pi N\Delta$ coupling constant f_Δ is investigated. The reason for considering the departure from the vacuum value is that a detailed study [29] of nuclear photo-absorption strongly favors such a change, more precisely a reduction of the f_Δ coupling by about (10–15)% at nucleon densities close to saturation. As expected a reduction of the coupling leads to a reduction of the isobar width. In the pion spectral function we can, at least for intermediate momenta, distinguish three branches. These are the main pion mode as well as the particle-hole and Δ-hole excitation. At about 0.3 GeV momentum we observe the level crossing between the main pion mode and the isobar-hole excitation. Decreasing f_Δ reduces the strength of the isobar-hole branch and in addition due to the narrower isobar that mode becomes better visible.

Next we study the influence of Migdal's g'_{22} parameter. Varying its value from 0.2 to 0.5 we arrive at the results shown in Fig. 7. The effect of changing g'_{22} is subtle since it influences the dressing of the isobar through the $\pi N\Delta$ vertex correction and also the pion self-energy by affecting the isobar-hole loop contribution. Increasing the value of g'_{22} softens the isobar and decreases its width, which compensates in part the reduction of the isobar-hole-loop contribution to the pion self-energy. All together the resulting change in the pion spectral function is modest. We note that a variation of g'_{12} is quite similar to that of g'_{22}. A variation of g'_{11} just affects the nucleon-hole contribution. Lowering g'_{11} makes the nucleon-hole branch of the pion larger, which in turn somewhat increases the isobar broadening.

We conclude with a discussion of the influence of the isobar mean field parameters. Results are shown for two parameter sets, which induce the same energy shift at zero momentum. Next to our standard set we use a set whose scalar mean field is put to zero and the vector part provides the net repulsion of 0.14 GeV at zero momentum as is implied also by Eq. (47). The effects can be found in Fig. 8. Without the scalar mean field we obtain less attraction at nonzero momentum and in addition the width of the isobar is significantly increased at larger momenta. This implies a smaller contribution of the isobar-hole state to the self-energy of the pion as shown in the lower right-hand panel of Fig. 8.

VIII. SUMMARY

A detailed study of pion and isobar properties in cold nuclear was presented. A fully relativistic and self-consistent

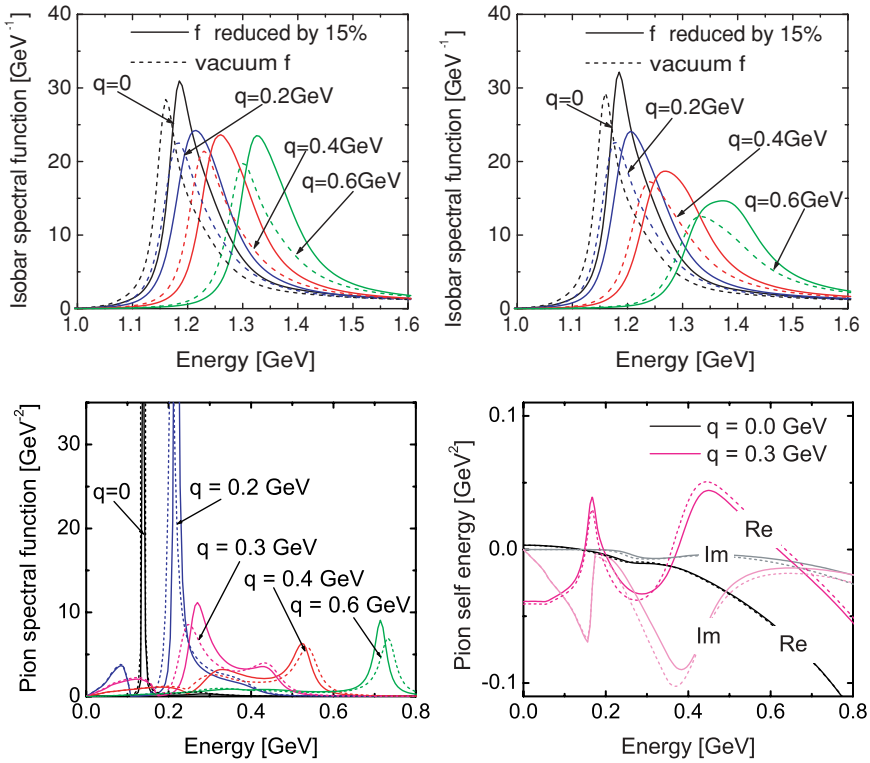

FIG. 6. (Color online) Same as Fig. 4, but varying the $\pi N\Delta$ coupling constant f_Δ. The solid lines correspond to the 15% reduction of f_Δ, the dashed ones to its free-space value.

many-body approach was developed that is applicable in the presence of Migdal's short-range correlations effects. Nuclear saturation and binding effects were modeled by scalar and vector mean fields for the nucleon. The novel subtraction scheme, that was constructed recently by two of the authors and that avoids the occurrence of kinematical singularities, was used. Unlike in previous studies no soft form factors for the $\pi N\Delta$ vertex were needed. For the first time the $\pi N\Delta$ vertex corrections as dictated by Migdal's short-range interactions were considered in a relativistic and self-consistent many-body approach. The latter were found to affect the isobar and pion properties dramatically. Using realistic parameter sets we

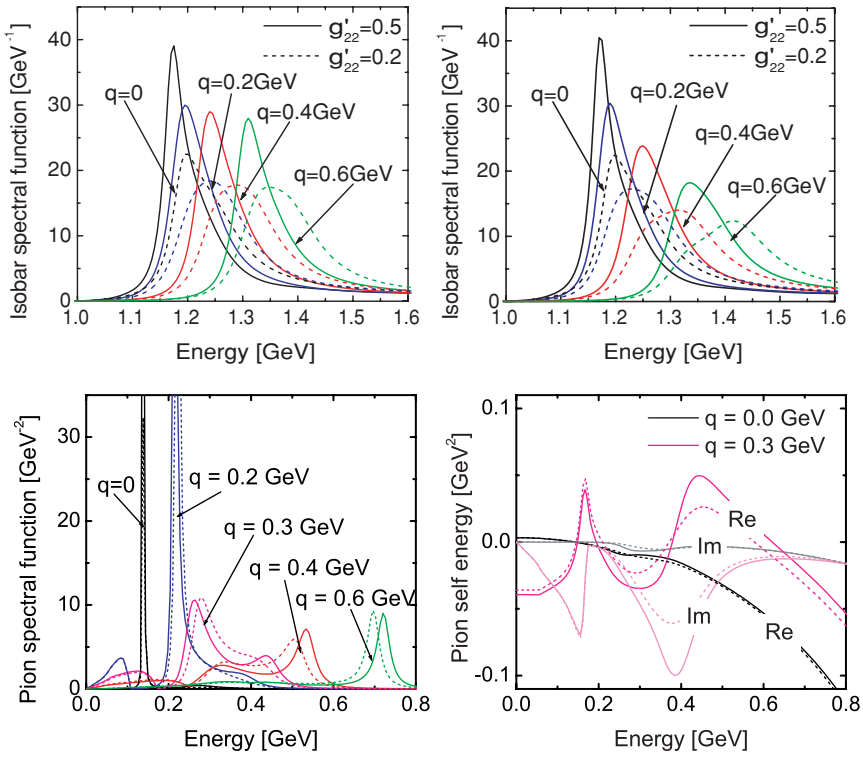

FIG. 7. (Color online) Same as Fig. 4 but for different values of the g'_{22} parameter. The solid lines correspond to the $g'_{22} = 0.5$, the dashed ones to $g'_{22} = 0.2$.

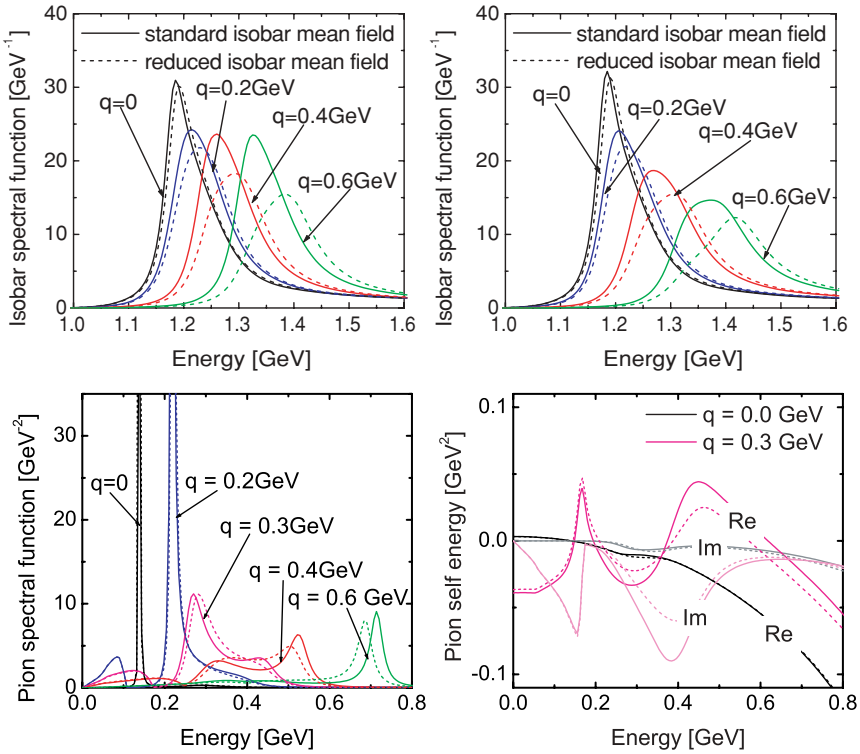

FIG. 8. (Color online) Same as Fig. 4 but for a variation of the delta mean-fields Σ_S^Δ and Σ_V^Δ. The solid lines correspond to the standard choice of Eq. (47), the dashed lines to the choice $\Sigma_S^\Delta = 0.00$ GeV and $\Sigma_V^\Delta = 0.14$ GeV.

predict a downward shift of about 50 MeV for the Δ resonance at nuclear saturation density. The pionic soft modes are much less pronounced than in previous studies.

Further studies are needed to consolidate our results. In particular an application to the pion-nucleus problem and the pionic atom data set would be useful to further constrain the parameter set. Our computation may be generalized to study effects of finite temperature.

ACKNOWLEDGMENTS

This research was supported in part by the Hungarian Research Foundation (OTKA) grant 71989. M.F.M.L. acknowledges stimulating discussions with R. Rapp and D. Voskresensky. C.L.K. would like to thank the G.S.I. (Darmstadt) and the K.V.I. (Groningen) for the kind hospitality. F.R. acknowledges useful discussions with J. Knoll and thanks the FIAS (Frankfurt) for support.

APPENDIX A

We present explicit representations for the nucleon- and isobar-hole loops introduced in Eq. (7) for the case of nuclear matter at rest with $u_\mu = (1, \vec{0})$. The longitudinal [20] and transverse nucleon-hole loop functions are

$$\Pi_{ij}^{(Nh)}(\omega,\vec{q}) = \frac{f_N^2}{m_\pi^2}\mathcal{P}\int_0^{k_F}\frac{d^3p}{2\,p_0\,(2\pi)^3}\,\frac{8\,K_{ij}^{(Nh)}}{2\,p\cdot q+q^2+i\,\epsilon} + \frac{i\,f_N^2}{m_\pi^2}\Im\int_0^{k_F}\frac{d^3p}{2\,p_0\,(2\pi)^3} \times\frac{8\,K_{ij}^{(Nh)}\,\Theta(k_F-|\vec{p}+\vec{q}\,|)}{2\,p\cdot q+q^2+i\,\epsilon}\,\Theta(p_0+\omega) + (-1)^{i+j}(q_\mu\to -q_\mu), \tag{A1}$$

where $q_\mu = (\omega, \vec{q}\,)$, $p_0 = \sqrt{m_N^2+\vec{p}^{\,2}}$, and

$$K_{11}^{(Nh)} = 2\,m_N^2,\quad K_{12}^{(Nh)} = K_{21}^{(Nh)} = 0,$$
$$K_{22}^{(Nh)} = \frac{\omega^2-\vec{q}^{\,2}}{\vec{q}^{\,2}}\,(2\vec{p}^{\,2}+\omega p_0+\vec{p}\cdot\vec{q})+2\,m_N^2\,\frac{\omega^2}{\vec{q}^{\,2}}, \tag{A2}$$
$$K_T^{(Nh)} = 3\,m_N^2+\omega p_0-\vec{p}\cdot\vec{q}-\frac{1}{2}\left(K_{11}^{(Nh)}+K_{22}^{(Nh)}\right).$$

Note that there is no appearance of the vector mean field parameter Σ_V.

For a bare isobar propagator, $S_0^{\mu\nu}(w)$ as given in Eq. (6), the longitudinal isobar-hole loop functions were computed already in [20]. We present here longitudinal as well as the transverse loop functions:

$$\Pi_{ij}^{(\Delta h)}(\omega,\vec{q}) = \frac{4}{9}\frac{f_\Delta^2}{m_\pi^2}\int_0^{k_F}\frac{d^3p}{2\,(p_0-\Sigma_V)\,(2\pi)^3} \times\frac{8\,K_{ij}^{(\Delta h)}\left(m_N\,m_\Delta+m_N^2+(p\cdot q)\right)}{2\,p\cdot q+q^2-m_\Delta^2+m_N^2+i\,\epsilon} + (-1)^{i+j}(q_\mu\to -q_\mu),$$
$$K_{11}^{(\Delta h)} = 1-\frac{(q^2+p\cdot q)^2}{q^2\,m_\Delta^2},$$
$$K_{22}^{(\Delta h)} = 1+\frac{(\omega\,|\vec{p}\,|\,\cos(\vec{q}\,,\vec{p}\,)-|\vec{q}\,|\,p_0)^2}{m_\Delta^2\,q^2},$$
$$K_{12}^{(\Delta h)} = K_{21}^{(\Delta h)}$$

$$= i\,\frac{q^2+p\cdot q}{q^2\,m_\Delta^2}\,(|\vec q\,|\,p_0-\omega\,|\vec p\,|\,\cos(\vec q\,,\,\vec p\,)),$$

$$K_T^{(\Delta h)} = 2-\frac{(p+q)^2}{2\,m_\Delta^2}-\frac{1}{2}\,\big(K_{11}^{(\Delta h)}+K_{22}^{(\Delta h)}\big), \quad \text{(A3)}$$

where $q_\mu=(\omega,\vec q\,)$, $p_0=\sqrt{m_N^2+\vec p^{\,2}}+\Sigma_V$. Both representations (A1), (A3) are compatible with Eq. (13). On the other hand, only Eq. (A1) is consistent with Eq. (15). The asymptotic behavior of the isobar-hole loop as given in Eq. (A3) is at odds with the condition (15).

To derive the general results for the isobar-hole loop functions in the presence of self-energy effects it is necessary to establish a generalization of Eq. (A3). Without assuming a specific form of the isobar propagator we find

$$\begin{aligned}
\Pi_{11}^{(\Delta h)}(\omega,\vec q\,) &= \frac{1}{q^2}\,\Pi_1^{(\Delta h)}(\omega,\vec q\,),\\
\Pi_{12}^{(\Delta h)}(\omega,\vec q\,) &= \frac{1}{\sqrt{q^2-(q\cdot u)^2}}\\
&\quad\times\left(\frac{q\cdot u}{q^2}\,\Pi_1^{(\Delta h)}(\omega,\vec q\,)-\Pi_2^{(\Delta h)}(\omega,\vec q\,)\right),\\
\Pi_{22}^{(\Delta h)}(\omega,\vec q\,) &= \frac{q\cdot u}{q^2-(q\cdot u)^2}\\
&\quad\times\left(\frac{q\cdot u}{q^2}\,\Pi_1^{\Delta h}(\omega,\vec q\,)-2\,\Pi_2^{(\Delta h)}(\omega,\vec q\,)\right.\\
&\quad\left.+\frac{q^2}{q\cdot u}\,\Pi_3^{(\Delta h)}(\omega,\vec q\,)\right),\\
\Pi_T^{(\Delta h)}(\omega,\vec q\,) &= \frac{1}{2}\,\big(\Pi_4^{(\Delta h)}(\omega,\vec q\,)-\Pi_{11}^{(\Delta h)}(\omega,\vec q\,)\\
&\quad-\Pi_{22}^{(\Delta h)}(\omega,\vec q\,)\big)
\end{aligned} \quad \text{(A4)}$$

as a consequence of the decomposition (16). The merit of the representation (A4) lies in its simple realization of the constraint equations (13). The first condition is satisfied for any functions $\Pi_i(\omega,\vec q\,)$ that are regular at $q^2=0$. The second equation in Eq. (13) implies the following constraint:

$$\begin{aligned}
&\Pi_3(\omega,0)=\frac{1}{\omega^2}\,\Pi_1(\omega,0), \quad \Pi_2(\omega,0)=\frac{1}{\omega}\,\Pi_1(\omega,0),\\
&\Pi_4(\omega,0)=3\,\Pi_{22}(\omega,0)+\Pi_{11}(\omega,0),
\end{aligned} \quad \text{(A5)}$$

where we boosted into the rest frame of nuclear matter for convenience. Based on the representation (16) we define

$$\begin{aligned}
\Pi_i^{(\Delta h)}(\omega,\vec q\,) &= \left[\delta_{i4}\,\Pi_3^{(\Delta h)}(0,\vec q\,)\right.\\
&\quad-\frac{8}{3}\,\frac{f_\Delta^2}{m_\pi^2}\int_0^{k_F}\frac{d^3p}{2\,(p_0-\Sigma_V)\,(2\pi)^3}\\
&\quad\left.\times\int_{-\infty}^{+\infty}\frac{d\bar\omega}{\pi}\,\Big(\frac{\omega}{\bar\omega}\Big)^{n_i}\,\frac{\mathrm{sign}(\bar\omega)\,\Im S_i^{(\Delta h)}(\bar\omega,\vec q,\,\vec p)}{\bar\omega-\omega-i\,\bar\omega\,\epsilon}\right]\\
&\quad+(-1)^{\epsilon_i}(q_\mu\to-q_\mu),
\end{aligned} \quad \text{(A6)}$$

where $p_0=\sqrt{m_N^2+\vec p^{\,2}}+\Sigma_V$ and $\epsilon_{1,3,4}=0$ and $\epsilon_2=1$. Furthermore $n_{1,4}=2$ but $n_2=1$ and $n_3=0$. We assure that the definition (A6) leads to a polarization tensor compatible with all constraints (13), (15). This is a consequence of specific identities the integral kernels enjoy [see Eq. (A9)].

The integral kernels, $S_i^{(\Delta h)}(q,\,p,\,u)$, required in Eq. (A6) are covariant functions of the four-momenta q_μ, p_μ, and u_μ. Their evaluation requires the contraction of the isobar propagator, $S_{\mu\nu}(p+q,u)$, with the q_μ and u_μ [see Eqs. (7), (9)]. We express the four-vector u_μ, in terms of v_μ and $X_\mu(v,u)$,

$$u_\mu=-\sqrt{(\hat v\cdot u)^2-1}\,X_\mu(v,u)+(\hat v\cdot u)\,\hat v_\mu, \quad \text{(A7)}$$

since the contraction of the isobar propagator with v_μ and $X_\mu(v,u)$ leads to more transparent expressions. In particular we can take over the results from [28], where contractions of the isobar propagator with the latter four-vectors were computed already. The results were decomposed into the extended algebra of projectors (23), (25) introducing the invariant expansion coefficients $S_{[ij]}^{(a)}(v,u)$ and $S_{[ij]}^{(ab)}(v,u)$ with $a,b=v,x$.

We present the integral kernels of Eq. (A6), which have transparent representations in terms of the invariant functions introduced in Eq. (16) and $c_{[ij]}^{(p,q)}(q;v,u)$ of [28]. We establish

$$\begin{aligned}
S_1^{(\Delta h)} &= \sum_{i,j=3}^{8} c_{[ij]}^{(p)}\,S_{[ij]}^{(p)}+\sum_{i,j=1}^{2} c_{[ij]}^{(q)}\,S_{[ij]}^{(q)},\\
S_2^{(\Delta h)} &= \sum_{i=1}^{2}\sum_{j=3}^{8} c_{[ij]}^{(p)}\,\big[(\hat v\cdot u)\,S_{[ij]}^{(v)}-\sqrt{(\hat v\cdot u)^2-1}\,S_{[ij]}^{(x)}\big],\\
S_3^{(\Delta h)} &= \sum_{i,j=1}^{2} c_{[ij]}^{(p)}\big[(\hat v\cdot u)^2\,S_{[ij]}^{(vv)}+((\hat v\cdot u)^2-1)\,S_{[ij]}^{(xx)}\\
&\quad-(\hat v\cdot u)\sqrt{(\hat v\cdot u)^2-1}\,\big(S_{[ij]}^{(xv)}+S_{[ij]}^{(vx)}\big)\big],\\
S_4^{(\Delta h)} &= \sum_{i,j=1}^{2} c_{[ij]}^{(p)}\,S_{[ij]}^{(g)}.
\end{aligned} \quad \text{(A8)}$$

A straightforward computation reveals that the kernels $S_i^{(\Delta h)}$ are correlated at vanishing three-momentum $\vec q=0$. In this case it holds

$$\begin{aligned}
S_3^{(\Delta h)} &= \frac{1}{\omega^2}\,S_1^{(\Delta h)}, \quad S_2^{(\Delta h)}=\frac{1}{\omega}\,S_1^{(\Delta h)},\\
S_4^{(\Delta h)} &= 3\,S_3^{(\Delta h)}-\frac{2}{\omega^2}\,S_1^{(\Delta h)}\\
&\quad-3\,\frac{d}{d\vec q^{\,2}}\Big|_{\vec q=0}\big(S_1^{(\Delta h)}-2\,\omega\,S_2^{(\Delta h)}+\omega^2\,S_3^{(\Delta h)}\big),
\end{aligned} \quad \text{(A9)}$$

where we assumed an angle average, i.e., the presence of $d\Omega_{\vec q}$.

APPENDIX B

We derive

$$V^{(p)}_{[33]} = \frac{f^2_\Delta}{m^2_\pi}\left[\frac{2\,\delta_V\,\delta\,(m_\Delta + (\tilde{w}\cdot\hat{v}))}{9m^2_\Delta\left(m^2_\Delta - \tilde{w}^2\right)}\right], \quad V^{(p)}_{[34]} = \frac{i\,\delta\,f^2_\Delta}{m^2_\pi\,m^2_\Delta\sqrt{(u\cdot\hat{v})^2-1}}\left[\frac{-2\,\delta_V\,\delta}{9\left(m^2_\Delta - \tilde{w}^2\right)}\right],$$

$$V^{(p)}_{[35]} = \frac{f^2_\Delta}{\sqrt{3}\,m^2_\pi\,m^2_\Delta}\left[\frac{3m_\Delta\left(m^2_\Delta - (\tilde{w}\cdot\hat{v})^2\right) - \delta_V\,\delta\,(2\,(\tilde{w}\cdot\hat{v}) - m_\Delta)}{3\left(m^2_\Delta - \tilde{w}^2\right)}\right],$$

$$V^{(p)}_{[36]} = -V^{(p)}_{[45]} = \frac{i\,\delta\,f^2_\Delta}{m^2_\pi\,m^2_\Delta\sqrt{3(u\cdot\hat{v})^2-3}}\left[\frac{2\left(m^2_\Delta - (\tilde{w}\cdot\hat{v})^2\right)}{3\left(m^2_\Delta - \tilde{w}^2\right)}\right],$$

$$V^{(p)}_{[37]} = \frac{\sqrt{2}\,i\,\delta f^2_\Delta}{3m^2_\pi\,m^2_\Delta\,\sqrt{(u\cdot\hat{v})^2-1}}\left[\frac{3\,m_\Delta(m_\Delta + (\tilde{w}\cdot\hat{v})) + 2\,\delta_V\,\delta}{3\left(m^2_\Delta - \tilde{w}^2\right)}\right], \quad V^{(p)}_{[38]} = \frac{-f^2_\Delta\,\delta(\delta_V(1-(u\cdot\hat{v})^2)+3\delta)(m_\Delta - 2(\tilde{w}\cdot\hat{v}))}{9\sqrt{2}\,m^2_\pi\,m^2_\Delta\left(m^2_\Delta - \tilde{w}^2\right)(1-(u\cdot\hat{v})^2)},$$

$$V^{(p)}_{[44]} = \frac{f^2_\Delta}{m^2_\pi\,m^2_\Delta}\left[\frac{2\delta_V\,\delta\,((\tilde{w}\cdot\hat{v}) - m_\Delta)}{9\left(m^2_\Delta - \tilde{w}^2\right)}\right], \quad V^{(p)}_{[46]} = \frac{f^2_\Delta}{\sqrt{3}\,m^2_\pi\,m^2_\Delta}\left[\frac{-3m_\Delta\left(m^2_\Delta - (\tilde{w}\cdot\hat{v})^2\right) - \delta_V\,\delta\,(2\,(\tilde{w}\cdot\hat{v}) + m_\Delta)}{3\left(m^2_\Delta - \tilde{w}^2\right)}\right],$$

$$V^{(p)}_{[47]} = \frac{-f^2_\Delta\,\delta(\delta_V(1-(u\cdot\hat{v})^2)+3\delta)(m_\Delta + 2(\tilde{w}\cdot\hat{v}))}{9\sqrt{2}\,m^2_\pi\,m^2_\Delta\left(m^2_\Delta - \tilde{w}^2\right)(1-(u\cdot\hat{v})^2)}, \quad V^{(p)}_{[48]} = \frac{\sqrt{2}\,i\,\delta f^2_\Delta}{3\,m^2_\pi\,m^2_\Delta\,\sqrt{(u\cdot\hat{v})^2-1}}\left[\frac{3\,m_\Delta(m_\Delta - (\tilde{w}\cdot\hat{v})) + 2\,\delta_V\,\delta}{3\left(m^2_\Delta - \tilde{w}^2\right)}\right],$$

$$V^{(p)}_{[55]} = \frac{f^2_\Delta}{3\,m^2_\pi m^2_\Delta}\left[\frac{-2(m_\Delta - (\tilde{w}\cdot\hat{v}))(m_\Delta + (\tilde{w}\cdot\hat{v}))^2}{m^2_\Delta - \tilde{w}^2}\right], \quad V^{(p)}_{[56]} = \frac{i\,\delta\,f^2_\Delta}{m^2_\pi\,m^2_\Delta\sqrt{(u\cdot\hat{v})^2-1}}\left[\frac{-2\left(m^2_\Delta - (\tilde{w}\cdot\hat{v})^2\right)}{3\left(m^2_\Delta - \tilde{w}^2\right)}\right], \tag{B1}$$

$$V^{(p)}_{[57]} = -\frac{\sqrt{2}\,i\,\delta f^2_\Delta}{3\,\sqrt{3}\,m^2_\pi\,m^2_\Delta\,\sqrt{(u\cdot\hat{v})^2-1}}\left[\frac{m^2_\Delta + 3m_\Delta(\tilde{w}\cdot\hat{v}) + 2\,(\tilde{w}\cdot\hat{v})^2}{\left(m^2_\Delta - \tilde{w}^2\right)}\right], \quad V^{(p)}_{[58]} = \frac{f^2_\Delta\,\delta(\delta_V(1-(u\cdot\hat{v})^2)+3\delta)(m_\Delta - 2(\tilde{w}\cdot\hat{v}))}{3\sqrt{6}\,m^2_\pi\,m^2_\Delta\left(m^2_\Delta - \tilde{w}^2\right)(1-(u\cdot\hat{v})^2)},$$

$$V^{(p)}_{[66]} = \frac{f^2_\Delta}{3\,m^2_\pi m^2_\Delta}\left[\frac{-2(m_\Delta - (\tilde{w}\cdot\hat{v}))^2(m_\Delta + (\tilde{w}\cdot\hat{v}))}{m^2_\Delta - \tilde{w}^2}\right], \quad V^{(p)}_{[67]} = -\frac{f^2_\Delta\,\delta(\delta_V(1-(u\cdot\hat{v})^2)+3\delta)(m_\Delta + 2(\tilde{w}\cdot\hat{v}))}{3\sqrt{6}\,m^2_\pi\,m^2_\Delta\left(m^2_\Delta - \tilde{w}^2\right)(1-(u\cdot\hat{v})^2)},$$

$$V^{(p)}_{[68]} = \frac{\sqrt{2}\,i\,\delta f^2_\Delta}{3\,\sqrt{3}\,m^2_\pi\,m^2_\Delta\,\sqrt{(u\cdot\hat{v})^2-1}}\left[\frac{m^2_\Delta - 3m_\Delta(\tilde{w}\cdot\hat{v}) + 2\,(\tilde{w}\cdot\hat{v})^2}{\left(m^2_\Delta - \tilde{w}^2\right)}\right],$$

$$V^{(p)}_{[77]} = -\frac{f^2_\Delta\,(m_\Delta + (\tilde{w}\cdot\hat{v}))}{m^2_\pi\left(m^2_\Delta - \tilde{w}^2\right)} + \frac{f^2_\Delta\,\delta\,(3\delta(2m_\Delta + (\tilde{w}\cdot\hat{v})) + \delta_V\,((u\cdot\hat{v})^2-1)(2\,m_\Delta + (\tilde{w}\cdot\hat{v})))}{9\,m^2_\pi m^2_\Delta\left(m^2_\Delta - \tilde{w}^2\right)(1-(u\cdot\hat{v})^2)},$$

$$V^{(p)}_{[78]} = \frac{-i\delta f^2_\Delta\left(9\delta^2 + ((u\cdot\hat{v})^2-1)\left(-5\,\delta_V\,\delta + 3m^2_\Delta\right)\right)}{9\,m^2_\pi\,m^2_\Delta\left(m^2_\Delta - \tilde{w}^2\right)\sqrt{(u\cdot\hat{v})^2-1}^3},$$

$$V^{(p)}_{[88]} = -\frac{f^2_\Delta\,(m_\Delta - (\tilde{w}\cdot\hat{v}))}{m^2_\pi\left(m^2_\Delta - \tilde{w}^2\right)} + \frac{f^2_\Delta\,\delta\,(3\delta(2m_\Delta - (\tilde{w}\cdot\hat{v})) + \delta_V\,((u\cdot\hat{v})^2-1)\,(2\,m_\Delta - (\tilde{w}\cdot\hat{v})))}{9\,m^2_\pi m^2_\Delta\left(m^2_\Delta - \tilde{w}^2\right)(1-(u\cdot\hat{v})^2)},$$

$$V^{(q)}_{[11]} = \frac{f^2_\Delta\,(m_\Delta + (\tilde{w}\cdot\hat{v}))}{m^2_\pi\left(\tilde{w}^2 - m^2_\Delta\right)}, \quad V^{(q)}_{[22]} = \frac{f^2_\Delta\,(m_\Delta - (\tilde{w}\cdot\hat{v}))}{m^2_\pi\left(\tilde{w}^2 - m^2_\Delta\right)}, \quad V^{(q)}_{[12]} = \frac{i\,\delta\,f^2_\Delta}{m^2_\pi\left(\tilde{w}^2 - m^2_\Delta\right)\sqrt{(u\cdot\hat{v})^2-1}},$$

where

$$\tilde{w}_\mu = w_\mu - \Sigma^\Delta_V\,u_\mu, \quad \delta = (u\cdot\hat{v})(\tilde{w}\cdot\hat{v}) - (u\cdot\tilde{w}),$$
$$\delta_V = \Sigma^N_V - \Sigma^\Delta_V. \tag{B2}$$

[1] D. Campell, R. Dashen, and J. Manassash, Phys. Rev. D **12**, 979 (1975).
[2] E. Oset and W. Weise, Phys. Lett. **B60**, 141 (1976).
[3] A. B. Migdal, Rev. Mod. Phys. **50**, 107 (1978).
[4] E. Oset, H. Toki, and W. Weise, Phys. Rep. **83**, 281 (1982).
[5] A. M. Dyugaev, Sov. J. Nucl. Phys. **38**, 680 (1983).
[6] V. F. Dmitriev and T. Suzuki, Nucl. Phys. **A438**, 697 (1985).
[7] E. Oset and L. L. Salcedo, Nucl. Phys. **A468**, 631 (1987).
[8] A. B. Migdal *et al.*, Phys. Rep. **192**, 179 (1990).
[9] T. Udagawa, S.-W. Hong, and F. Osterfeld, Phys. Lett. **B245**, 1 (1990).
[10] J. Delorme and P. A. M. Guichon, Phys. Lett. **B263**, 157 (1991).
[11] T. Herbert, K. Wehrberger, and F. Beck, Nucl. Phys. **A541**, 699 (1992).
[12] R. C. Carrasco and E. Oset, Nucl. Phys. **A536**, 445 (1992).
[13] J. Nieves, E. Oset, and C. Garcia-Recio, Nucl. Phys. **A554**, 554 (1993).
[14] L. Xia, P. J. Siemens, and M. Soyeur, Nucl. Phys. **A578**, 493 (1994).
[15] P. Arve and J. Helgesson, Nucl. Phys. **A572**, 600 (1994).
[16] C. L. Korpa and R. Malfliet, Phys. Rev. C **52**, 2756 (1995).
[17] H. Kim, S. Schramm, and S. H. Lee, Phys. Rev. C **56**, 1582 (1997).
[18] R. Rapp, M. Urban, M. Buballa, and J. Wambach, Phys. Lett. **B417**, 1 (1998).
[19] M. Nakano *et al.*, Int. J. Mod. Phys. E **10**, 459 (2001).
[20] M. F. M. Lutz, Phys. Lett. **B552**, 159 (2003); **B566**, 277(E) (2003).
[21] C. L. Korpa and M. F. M. Lutz, Nucl. Phys. **A742**, 305 (2004).
[22] M. Post, S. Leupold, and U. Mosel, Nucl. Phys. **A741**, 81 (2004).
[23] F. Riek and J. Knoll, Nucl. Phys. **A740**, 287 (2004).
[24] C. L. Korpa and A. E. L. Dieperink, Phys. Rev. C **70**, 015207 (2004).
[25] H. van Hees and R. Rapp, Phys. Lett. **B606**, 59 (2005).
[26] M. F. M. Lutz and E. E. Kolomeitsev, Nucl. Phys. **A700**, 193 (2002).
[27] M. F. M. Lutz and C. L. Korpa, Nucl. Phys. **A700**, 309 (2002).
[28] M. F. M. Lutz, C. L. Korpa, and M. Möller, Nucl. Phys. **A808**, 124 (2008).
[29] F. Riek, M. F. M. Lutz, and C. L. Korpa, Phys. Rev. C **80**, 024902 (2009).
[30] M. Hirata, J. H. Koch, F. Lenz, and E. J. Moniz, Ann. Phys. (NY) **120**, 205 (1979).
[31] J. Ahrens *et al.*, Phys. Lett. **B146**, 303 (1984); N. Bianchi *et al.*, *ibid.* **B299**, 219 (1993); Th. Frommhold *et al.*, Z. Phys. A **350**, 249 (1994); N. Bianchi *et al.*, Phys. Rev. C **54**, 1688 (1996).
[32] T. Wakasa *et al.*, Phys. Rev. C **55**, 2909 (1997).
[33] SAID online program, http://gwdac.phys.gwu.edu/.
[34] A. Ramos and E. Oset, Nucl. Phys. **A671**, 481 (2000).